

# Frustration and Multicriticality in the Antiferromagnetic Spin-1 Chain

J. H. Pixley,<sup>1</sup> Aditya Shashi,<sup>1,2</sup> and Andriy H. Nevidomskyy\*<sup>1</sup>

<sup>1</sup>*Department of Physics and Astronomy, Rice University, Houston, Texas, 77005, USA*

<sup>2</sup>*Department of Physics, Harvard University, Cambridge, Massachusetts 02138, USA*

(Dated: December 3, 2024)

We consider the spin  $S = 1$  Heisenberg chain, with nearest neighbor, next nearest neighbor ( $\alpha$ ) and biquadratic ( $\beta$ ) interactions using a combination of the density matrix renormalization group (DMRG), a variational matrix product state wave function, and non-Abelian bosonization. We study the effect of frustration ( $\alpha > 0$ ) on the Haldane phase with  $-1 \leq \beta < 1$  which reveals a rich phase diagram. For  $-1 < \beta < \beta^*$ , we establish the existence of a spontaneously dimerized phase for large  $\alpha > \alpha_c$ , separated from the Haldane phase by the critical line  $\alpha_c(\beta)$  of second-order phase transitions connected to the Takhtajan–Babujian integrable point  $\alpha_c(\beta = -1) = 0$ . In the opposite regime,  $\beta > \beta^*$ , the transition from the Haldane phase becomes first-order into the next nearest neighbor (NNN) AKLT phase. Based on field theoretical arguments and DMRG calculations we conjecture these two regimes are separated by a multi-critical end-point  $(\beta^*, \alpha^*)$  of a different universality class, described by the  $SU(2)_4$  Wess–Zumino–Witten critical theory. From the DMRG calculations we estimate this end-point to lie in the range  $-0.2 < \beta^* < -0.15$  and  $0.47 < \alpha^* < 0.53$ . For large frustration above the critical line  $\alpha > \alpha_c(\beta)$ , we find that the dimerized phase smoothly crosses over to the NNN AKLT phase via an intermediate dimer phase with incommensurate short range order. We show the existence of two incommensurate crossovers: the Lifshitz transition and the disorder transition of the first kind, marking incommensurate correlations in momentum and real space, respectively. We show these crossover lines stretch across the entire  $(\beta, \alpha)$  phase diagram, merging into a single incommensurate-to-commensurate transition line for negative  $\beta \lesssim \beta^*$ .

PACS numbers: 75.10.Jm, 75.10.Kt, 75.10.Pq

## I. INTRODUCTION

Quantum spin chains prominently display new phases and quantum phase transitions that emerge from the interplay of quantum and thermal fluctuations, geometrical frustration, and strong interactions.<sup>1</sup> A variety of compounds can be modeled as quantum spin chains, such as  $\text{Ni}(\text{C}_2\text{H}_8\text{N}_2)_2\text{NO}_2\text{ClO}_4$  (NENP) [Ref. 2] and  $\text{CsNiCl}_3$  [Ref. 3] which realize antiferromagnetic spin  $S = 1$  Heisenberg chains, as well as  $f$ -electron compounds, like  $\text{Yb}_4\text{As}_3$ , representing the one dimensional spin-1/2 antiferromagnet<sup>4</sup>. More recently in systems of ultra-cold atoms, there are now proposals to realize spin chains using spinor atoms in an optical lattice<sup>5–7</sup>. It is crucial to understand the role of geometrical frustration and competing interactions, which can be engineered artificially in cold atom systems, and appear naturally in the strong coupling approach to e.g. the high temperature copper oxide and iron pnictide superconductors. For instance, it was shown that doping away from half-filling introduces frustration into the superexchange spin interaction<sup>8</sup> in the cuprates, whereas the biquadratic spin-spin interaction  $(\mathbf{S}_i \cdot \mathbf{S}_j)^2$  arises naturally within the spin  $S = 1$  Heisenberg model describing the strong coupling theory of the iron pnictides<sup>9</sup>.

We know from Haldane’s mapping of the spin chain onto the non-linear sigma model<sup>10</sup> that the behavior of

half-integer and integer spin- $S$  chains are dramatically different: the former possess gapless spinon excitations and quasi-long-range order<sup>14</sup>, whereas the spectrum of the latter is gapped with only short-range magnetic order. While the role of frustration has been studied extensively in the half-integer (in particular  $S = 1/2$ ) spin chains, its role in the integer spin case has been less well studied. Naturally, the simplest integer case is the  $S = 1$  spin chain, and this is the central focus of the present work, motivated in part by the aforementioned experimental realizations<sup>2,3</sup>.

Perhaps the simplest frustrated model is the isotropic Heisenberg quantum spin chain with antiferromagnetic nearest neighbor and next nearest neighbor (NNN) interactions. Previous DMRG studies<sup>11,12</sup> of such a frustrated  $S = 1$  chain indicate that there is a first-order phase transition from the Haldane phase into the so-called next-nearest neighbor Affleck–Kennedy–Lieb–Tasaki (NNN-AKLT) phase characterized by singlet links along the NNN bonds, see Fig. 1. Both the Haldane and NNN-AKLT phases are gapped, and the scenario of the first-order phase transition agrees with the field-theoretical analysis<sup>13</sup> concluding that the spectral gap does not close for arbitrary values of the next-nearest neighbor interaction. Another way to introduce frustration is by adding a competing biquadratic spin-spin interaction  $(\mathbf{S}_i \cdot \mathbf{S}_j)^2$  into the model. It turns out that this results in a significantly richer phase diagram harboring a variety of quantum phases, both gapped and gapless, which have been studied extensively in the past<sup>15–21,25</sup>. However, to the best of our knowledge, the combined effect of both the NNN and biquadratic interactions has not been studied

\*nevidomskyy@rice.edu

previously, and this is the subject of the present work. We therefore consider the most general spin  $S = 1$  chain with both types of frustration present:

$$H = J_1 \left[ \sum_i \mathbf{S}_i \cdot \mathbf{S}_{i+1} + \alpha \mathbf{S}_i \cdot \mathbf{S}_{i+2} + \beta (\mathbf{S}_i \cdot \mathbf{S}_{i+1})^2 \right] \quad (1)$$

We shall only consider the antiferromagnetic case ( $J_1 > 0$ ,  $\alpha > 0$ ), with the aim to study the effect of frustration in the region  $-1 \leq \beta < 1$ . Below we shall first summarize the known theoretical results for the spin-1 chain in this regime.

The bilinear-biquadratic model with  $\alpha = 0$  has been studied extensively. As already mentioned, the isotropic NN spin model ( $\beta = 0$ ) lies in the *Haldane phase*, characterized by exponentially decaying spin correlations and a gapped excitation spectrum, in stark contrast to antiferromagnets in higher dimension which display long range order and gapless spin-wave excitations, or half-integer spin chains as we have previously mentioned. The Haldane phase turns out to be stable for finite values of  $\beta$  in the range  $-1 < \beta < 1$ , with a singlet ground state in the thermodynamic limit<sup>15</sup> and a finite string order parameter signifying the spontaneous breakdown of the hidden  $Z_2 \times Z_2$  symmetry<sup>16</sup>. In an open chain, the ground state is four-fold degenerate, due to the first excited triplet of the effective spin-1/2 edge excitations (“Kennedy triplet”<sup>17</sup>) becoming degenerate with the singlet ground state. These edge excitations are the simplest example of gapless edge states, which are a consequence of the topologically non-trivial ground state in the bulk. A special case of  $\beta = 1/3$  has been analyzed by Affleck, Kennedy, Lieb and Tasaki (AKLT)<sup>18</sup>, who found an exact ground state to be of the valence-bond-solid (VBS) type. In the following, we refer to this as the AKLT point. It turns out that this point also marks the onset of incommensurability in the real-space spin-spin correlations, and falls into the classification of the *disorder transition of the first kind*<sup>29</sup> (see section V for more details). For larger values of positive  $\beta$ , one finds a Lifshitz transition at  $\beta_L = 0.43806(4)$  [Ref. 39] where the spin structure factor  $S(q)$  develops a double-peak structure at incommensurate momenta.

For  $\beta < -1$  and  $\alpha = 0$ , the system is in the dimerized ground state (see Fig. 1), which is two-fold degenerate in the thermodynamic limit due to the two different possible dimer coverings of the chain. The dimer state has a finite gap<sup>19–21</sup> (see Fig. 1) and has a unique ground state for an open chain with even number of sites. The point  $\beta = -1$  at which the transition occurs turns out to be exactly solvable<sup>22,23</sup> and is known as the Takhtajan–Babudjian (TB) point, described by the critical  $SU(2)_{k=2}$  Wess–Zumino–Witten (WZW) conformal field theory<sup>24</sup>. On the positive  $\beta$  side, the Haldane phase is flanked by a gapless phase with antiferro-quadrupolar quasi-long range order<sup>25</sup> for  $\beta > 1$ . The transition between the two is marked by the exactly solvable Uimin–Lai–Sutherland (ULS) point<sup>26</sup> at  $\beta = 1$ . In this work, we limit the discussion to the dimerized and Haldane phases and do not

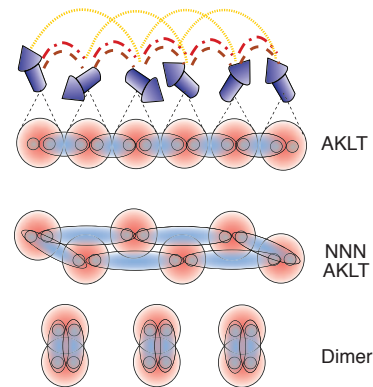


FIG. 1: (Color online) Schematic rendering of spin-1 chain with nearest (brown dashed), next-nearest (yellow dashed), and biquadratic (red dashed) interactions. Three “typical” ground states (GS) illustrated corresponding to the AKLT state, which is the exact GS at  $\beta = 1/3, \alpha = 0$ , the “next-nearest-neighbor” AKLT (NNN-AKLT) which takes over for large  $\alpha$ , and the dimerized states characteristic of  $\beta < -1$ . We complement numerical studies of the model with a variational wavefunction represented as a matrix product state which interpolates the three states described above.

consider the regime  $\beta > 1$ . The effect of frustration on the ULS point due to NNN interactions is left for future study.

As the reader can see, the spin-1 chain with  $\alpha = 0$  has a venerable history. The effect of NNN interactions ( $\alpha > 0$ ) on the other hand, has scarcely been studied. To the best of our knowledge, only the case of vanishing biquadratic interaction  $\beta = 0$  has been addressed. In this case, the authors of Refs. 11,12 found, using a combination of DMRG calculations and a variational wavefunction approach, that the VBS phase is stable for  $\alpha$  in the range  $\alpha < \alpha_T$  and that the AKLT wave function still provides a good description of the ground state. We will therefore refer to this VBS state as the “AKLT state” in what follows, even though it spans a much broader region around the AKLT point ( $\beta = 1/3, \alpha = 0$ ) originally studied in Ref. 18. Similar to the pure biquadratic model, disorder and Lifshitz points were found at  $\alpha_d = 0.284(1)$  and  $\alpha_L = 0.3725(25)$ , respectively<sup>11,12</sup> (see section V for more detail). Intriguingly, for larger values of  $\alpha$ , there is a phase transition at  $\alpha_T = 0.7444(6)$  from the AKLT phase to the so-called next nearest neighbor AKLT (NNN-AKLT) phase<sup>11,12</sup> illustrated in Fig. 1. At the transition, the DMRG calculations showed<sup>11,12</sup> that the gap remains finite, in agreement with earlier field-theoretical calculations.<sup>13</sup> Although the DMRG calculations in Refs. 11,12 do not find a discontinuous first derivative of the ground state energy at the transition, the authors concluded the transition to be first order, based on the finite jump of the string order parameter at  $\alpha_T$ . In the following, whenever we refer to a first order transition between the AKLT and NNN AKLT phases, this is the transition we have in mind. The disappearance of the string order parameter above  $\alpha_T$ , together with the gapping out of the edge

excitations, imply that this transition is topological in nature, from the topological AKLT phase into a topologically trivial NNN-AKLT phase where the  $Z_2 \times Z_2$  symmetry is restored<sup>11,12</sup>.

The above findings along the  $\beta = 0$  axis suggest that the NNN interaction  $\alpha$  has a profound effect on the ground state of spin-1 chain, yet virtually nothing is known about its phase diagram when both  $\alpha$  and  $\beta$  are finite. In this work, we aim to fill in this gap while attempting to address the following main questions:

- What is the topology of the phase diagram in the  $(\beta, \alpha)$  plane? Are all transitions first order as in the  $\beta = 0$  case?
- What happens in the vicinity of the gapless TB point ( $\beta = -1, \alpha = 0$ ) for finite  $\alpha$ ? Does the gapless behavior survive for a range of  $\alpha$ , or is an infinitesimal value of  $\alpha$  sufficient to gap out the spectrum?
- How are the dimerized and the NNN-AKLT phases connected? Is there a phase transition between the two?
- How does the incommensurability of spin-spin correlations set in? What is the significance of the AKLT point ( $\beta = 1/3$ ) in the presence of a finite NNN interaction  $\alpha$ ?
- Can one obtain a realistic description of the system using a variational wave function based on matrix product states, shown to work successfully<sup>12</sup> for  $\beta = 0$ ?

The remainder of the paper is organized as follows. We first state our main results by illustrating the topology of the phase diagram in section II. Next, we discuss the emergence of a line of critical points in the vicinity of the TB point, whose existence we verify using conformal field-theory arguments, in section III. We then discuss each phase comprehensively, and outline the details of the DMRG and variational wave function approaches used to obtain them in section IV. The nature of the incommensurability in the spin-spin correlations is examined in detail in section V and the short range phase diagram is constructed. We discuss the results and future directions in section VI. We conclude with a summary of the results in section VII and section VIII contains the technical details of the various methods used in this work.

## II. PHASE DIAGRAM

Our results can be most clearly stated by first presenting a schematic phase diagram in figure 2. Using a combination of field theoretical arguments and DMRG calculations guided by a MPS wave function approach, we find the existence of a critical line,  $\alpha_c(\beta)$  in figure 2. The critical line starts at the TB point and terminates at a multicritical endpoint  $\Omega = (\beta^*, \alpha^*)$  turning into a line of first order transitions  $\alpha_T(\beta)$ , smoothly connected

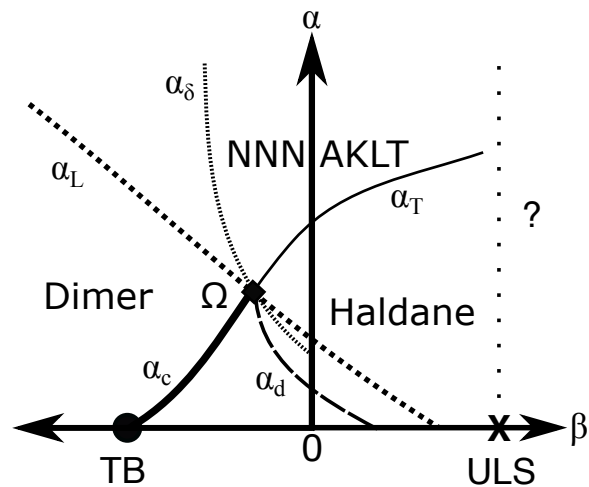


FIG. 2: Schematic phase diagram obtained in this work. The critical line (thick black line)  $\alpha_c(\beta)$  starts at the TB point, and is terminated at a multi-critical point  $\Omega$ , after which the transition becomes first order (thin black line  $\alpha_T$ ). The critical line separates the dimer and Haldane phases whereas transition line separates the Haldane and NNN AKLT phases. The medium dashed black line is the Lifshitz line  $\alpha_L(\beta)$  that merges with the disorder line ( $\alpha_d(\beta)$ , long black dashed) above the critical line. The small dashed line  $\alpha_\delta(\beta)$ , marks the cross over to the NNN AKLT phase when above the critical line. We have not studied the effect of  $\alpha$  on the region  $\beta \geq 1$  and therefore denote this with a question mark.

to the first order transition at  $\alpha_T(\beta = 0) = 0.7444(6)$  (Refs. 11,12). The line of first order transitions extends into the region  $0 < \beta < 1$  for finite  $\alpha$ , we refer to this line of first order transitions as the “transition” line. We find the critical and transition lines separates the AKLT phase with a phase that breaks the translational symmetry of the lattice, we refer to this entire phase as the translational symmetry broken phase (TSBP). We find the TSBP can be divided into three regions, the dimer and NNN AKLT phases that are connected by an incommensurate dimer phase (the region between the dimer and NNN AKLT phases in figure 2). Above the transition, for  $\alpha > \alpha_c(\beta)$  and  $\alpha > \alpha_T(\beta)$ , we find that the edge excitations become gapped out, implying that the topological nature of the ground state in the Haldane phase changes to being topologically trivial in the TSBP.

The existence of the TSBP is quite natural after considering two limiting cases of the Hamiltonian in equation (1). First, in the limit  $\beta \rightarrow -\infty$ , we can drop the nearest and next nearest neighbor Heisenberg interactions and the model reduces to the purely biquadratic model with negative  $\beta$ . This problem has been studied previously and is known to be in a spontaneously dimerized ground state and is exactly solvable via Bethe ansatz<sup>27</sup>. The dimerized ground state breaks the translational symmetry of the lattice because only every other bond is now equivalent, see figure 1. In the opposite limit  $\alpha \rightarrow \infty$ , we have two decoupled antiferromagnetic spin-1 chains with a doubled lattice spacing of the original problem. There-

fore, as we will show concretely using the DMRG, even though the character of the wave function is different in the dimerized and NNN AKLT phases, they cannot be distinguished on symmetry grounds alone and must therefore be smoothly connected via a series of crossovers, shown schematically as the dashed lines  $\alpha_L$  and  $\alpha_\delta$  in figure 2 (the precise physical meaning of these crossovers are discussed in detail in sections IV and V).

In addition, we use the DMRG to study the short range nature of the phase diagram. By considering the spin-spin correlation function, we find lines of disorder [ $\alpha_d(\beta)$ ] and Lifshitz points [ $\alpha_L(\beta)$ ] where incommensurate correlations develop in real and momentum space respectively. We find that these two lines of transitions merge into a single line upon entering the translational-symmetry broken phase, similar to what has been seen in frustrated classical two dimensional Heisenberg models (see figure 14(c)). Intriguingly, to the accuracy of our finite-size DMRG calculations, we find the location of the multi-critical endpoint  $\Omega$  to lie at the intersection of the disorder  $\alpha_d$ , Lifshitz  $\alpha_L$ , and critical  $\alpha_c$  lines, as Figure 2 illustrates.

### III. CRITICAL LINE

#### A. Field Theoretical Picture

##### 1. Non-Abelian bosonization of $S=1$ chain

We first focus on the phase boundary between the dimer and Haldane phases, shown as the thick solid black line in Fig. 2. It is instructive to consider the vicinity of the integrable TB point ( $\beta = -1$ ), which is equivalent in the continuum limit to a level-2  $SU(2)$  Wess-Zumino-Witten (WZW) model<sup>24</sup>. The fundamental question is what happens to this critical point in the phase space of parameters  $(\beta, \alpha)$  of the Hamiltonian Eq. (1). It would seem that there could be two possibilities: (a) either both the next-nearest neighbour interaction  $\alpha(\mathbf{S}_i \cdot \mathbf{S}_{i+2})$  and the biquadratic interaction  $\beta(\mathbf{S}_i \cdot \mathbf{S}_{i+1})^2$  turn out to be relevant and thus open up a gap in the spectrum of excitations, or (b) there is an irrelevant direction in the  $(\beta, \alpha)$  plane that leaves the system critical, in which case the resulting theory ought to be described by a conformal field theory. Which of these two possibilities is realized?

In order to answer this question, we must understand how the integrable TB point can be perturbed, and for this we must consider all allowed perturbations of the corresponding WZW theory. This seemingly impossible task is achievable by virtue of the conformal field theory, which dictates that all perturbing fields can be expressed in terms of the primary conformal fields. The  $SU(2)_2$  theory is characterized by two non-trivial representations of bilinears built from primary fields: the doublet  $g_{mn}$  with conformal dimensions  $(\frac{3}{16}, \frac{3}{16})$ , which transforms in the fundamental representation of  $SU(2)$ , and the triplet  $\Phi_{ab}$  with conformal dimensions  $(\frac{1}{2}, \frac{1}{2})$ ,

which transforms in the 3-dimensional adjoint representation. All possible perturbations to the WZW theory can be constructed from these two scaling fields and their conformal descendants, in addition to the bilinear of primary currents  $(J^a \bar{J}^a)$ . It was shown by Affleck and Haldane<sup>24</sup> that the scaling field  $g_{mn}$  is proportional to the staggered magnetization  $(-1)^i \mathbf{S}_i \cdot \mathbf{S}_{i+1}$  and is therefore not allowed to appear as a perturbation, because it would otherwise explicitly break the translational symmetry of the chain. We thus conclude that small deviations from the TB point can be described, in the continuum limit, by the Lagrangian of the  $SU(2)_2$  WZW theory plus the following perturbations:

$$\mathcal{L} = \mathcal{L}_{\text{WZW}} + m \text{Tr}(\hat{\Phi}) - \lambda J^a \bar{J}^a, \quad (2)$$

(summation implied over field components  $a = 1, 2, 3$ ).

The  $\text{Tr}(\hat{\Phi})$  term has scaling dimension  $\Delta = 1$  and is strongly relevant in (1+1) dimension, leading to the opening of the spin gap. Depending on the sign of the ‘‘mass’’  $m$ , the system ends up either in the Haldane phase ( $m < 0$ ) or in the symmetry-breaking dimerized phase ( $m > 0$ ). In fact, for  $\alpha = 0$ , the mass is proportional to the distance from the TB point<sup>24</sup>,  $m \propto -(1+\beta)$ . We note in passing that the dimer phase and the so-called next-nearest-neighbor AKLT (NNN-AKLT) phase<sup>11</sup> appear to be smoothly connected by a crossover rather than a phase transition, because both phases break translational symmetry and cannot be distinguished on symmetry grounds alone (see Section V C 2). For this reason, from the point of view of the conformal field theory, both the dimer phase and NNN-AKLT phase are reached by the massive perturbation  $m \text{Tr}(\hat{\Phi})$  with  $m > 0$ .

Let us now consider the last term in Eq. (2). It has a scaling dimension  $\Delta = 2$  and is marginal at the tree level. Higher order RG calculations show<sup>44</sup> that this term is marginally irrelevant for  $\lambda > 0$  (corresponding to the AFM sign of the nearest-neighbour interaction), whereas for negative  $\lambda$ , it becomes marginally relevant, flowing towards the dimerized state in strong coupling. The values of the parameters  $(m, \lambda)$  in the effective continuum theory (2) are related in some fashion to the parameters  $(\alpha, \beta)$  of the original Hamiltonian, although the exact correspondence is unknown. Nevertheless, the above scaling argument allows us to sketch the RG flow in the vicinity of the TB point, see Fig. 3. The solid black line is massless ( $m = 0$ ) and remains critical for  $\lambda > 0$  at least for small perturbations, with the critical exponents governed by the flow toward the integrable WZW  $SU(2)_2$  theory at the TB point (plus logarithmic corrections due to marginally irrelevant operators). Crossing the solid black line in figure 3 signifies the 2<sup>nd</sup> order phase transition between the Haldane phase and the dimerized (or NNN-AKLT) phase. This is indeed what our DMRG calculations show for  $\beta \lesssim -0.2$ , indicating a vanishing gap to the bulk excitations in the thermodynamic limit and diverging correlation length, see Fig. 4.

Intriguingly, in the absence of a biquadratic coupling,  $\beta = 0$ , Kolezhuk and co-workers argued that upon in-

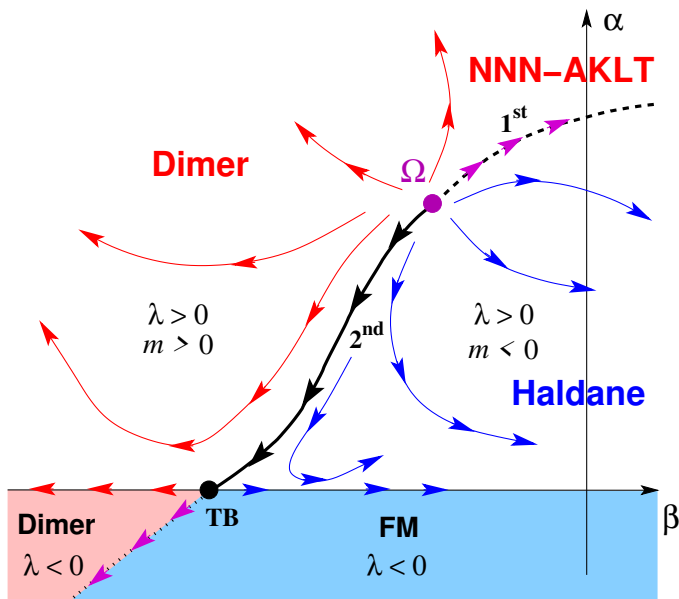


FIG. 3: (Color online) Schematic RG flow diagram in the vicinity of the Takhtajan–Babudjian (TB) point. The signs of conformal theory parameters  $m$  and  $\lambda$  in Eq. (2) determine the nature of the phases (Dimer, Haldane, or ferromagnet). The solid black line is critical and is governed by the conformal WZW theory at the TB point. We identify a critical end-point  $\Omega$ , characterized by an unstable RG flow, marking the 1<sup>st</sup> order phase transition everywhere along the dashed line (see text for discussion).

creasing  $\alpha$ , the transition from the Haldane phase to the dimerized NNN-AKLT phase is first-order, with the bulk gap never closing across the transition<sup>11,12</sup>. Our DMRG results corroborate this statement for  $\beta \geq 0$ , see Fig. 5. How do we reconcile the seemingly contradictory results in Figs. 4 and 5? Could the transition be first order throughout the phase diagram with a small gap which is below the DMRG detection threshold? Indeed, it is very difficult within DMRG to distinguish a system with a small but finite gap from a true gapless case, as the recent state-of-the-art DMRG studies on the kagomé lattice demonstrate<sup>45,46</sup>. Conversely, could it be that the true bulk gap does vanish across the transition, however the finite-size effects result in a numerically finite gap, even when extrapolated to  $L \rightarrow \infty$ ? Below we shall settle this ambiguity with the help of field-theoretical analysis. What we find is that the second-order transition for  $\beta \lesssim -0.2$  (see Fig. 4) and the apparent first-order transition for positive  $\beta$  (Fig. 5) are both correct, and that there exist a critical end-point  $\Omega$  terminating the line of the second-order transitions in the phase diagram Fig. 3.

## 2. Critical endpoint: Conformal field theory

Based on the DMRG results for the spectral gap and spin-spin correlation functions, we propose the existence

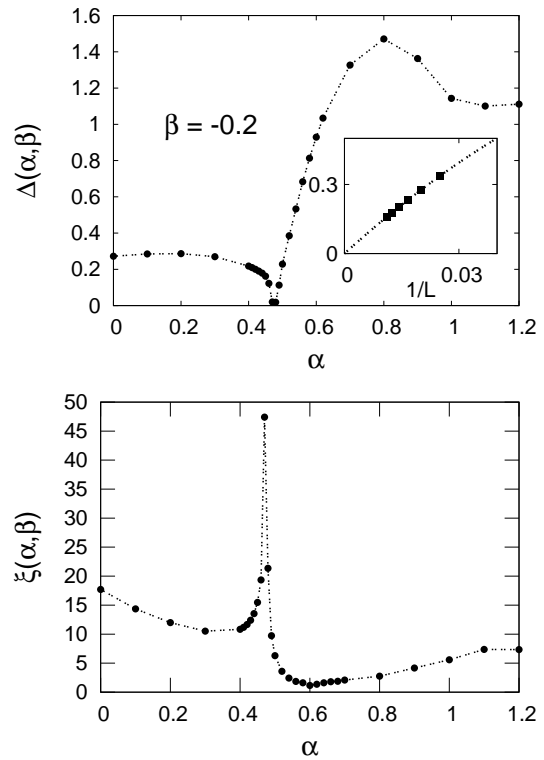


FIG. 4: Upper Plot: The bulk gap  $\Delta(\alpha, \beta)$  in the thermodynamic limit as a function of  $\alpha$  for  $\beta = -0.2$ . At the critical point  $\alpha_c(\beta = -0.2) = 0.480(5)$  we find a small gap  $\Delta(\alpha = 0.48, \beta = -0.2) = 0.019(3)$ . Inset: At the critical point, we find an excellent fit to a gapless form  $\Delta(L) = a_\Delta/L + b_\Delta/L^2$ . Lower Plot: Correlation length for a fixed system size  $L = 80$  [see equation (7) for a definition of  $\xi$ ], as we move through the critical line, with a disorder point at the minimum of  $\xi$  at  $\alpha_d(\beta = -0.2) = 0.600(5)$ .

of a critical end-point  $\Omega$  in the phase diagram Fig. 3. The continuum limit of this critical point must be described by a conformal field theory, however it becomes quickly apparent that this cannot be the same  $SU(2)_2$  WZW theory that describes the TB point at  $\beta = -1$ . The fundamental reason is that as explained above, the  $SU(2)_2$  field theory has only one relevant operator: the mass term  $m\text{Tr}(\Phi)$  in Eq. (2). By contrast, the critical end-point  $\Omega$  must have two relevant (or marginally relevant) operators – one playing the role of the mass term that opens up the Haldane gap (blue and red flow lines in Fig. 3), and another one, which makes the critical point  $\Omega$  unstable towards the 1<sup>st</sup> order phase transition along the purple flow line in Fig. 3. In other words,  $\Omega$  must be an unstable fixed point in the  $(\alpha, \beta)$  phasespace, and this requires more than one relevant operator.

The sought conformal field theory must therefore be richer than the  $SU(2)_2$  theory and must satisfy the following requirements: (a) it must possess at least two relevant (or marginally relevant) scaling fields, as explained above; (b) it must satisfy Zamolodchikov’s “ $c$ -theorem”<sup>49</sup>, so that its central charge must monotonically

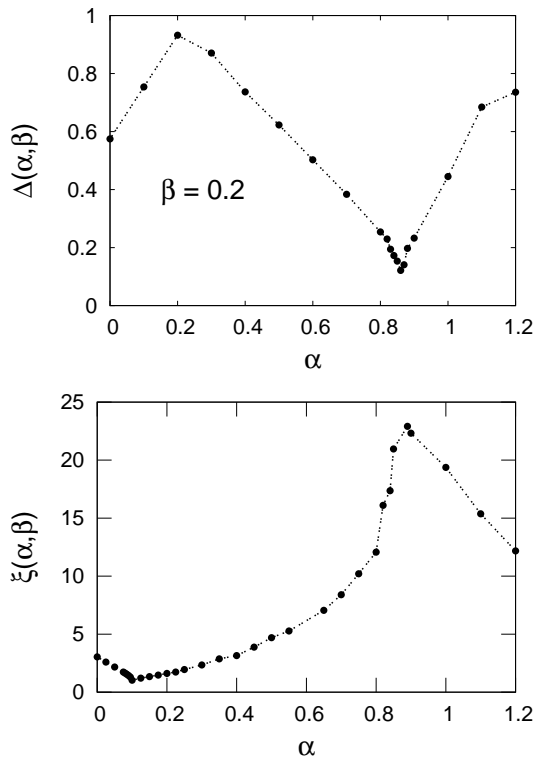


FIG. 5: Upper Plot: The bulk gap  $\Delta(\alpha, \beta)$  in the thermodynamic limit as a function of  $\alpha$  for  $\beta = 0.2$ ; we see that the gap goes through a minimum in the vicinity of  $\alpha_T(\beta = 0.2) = 0.855(5)$ , with a minimum value of  $\Delta(\alpha = 0.86, \beta = 0.2) = 0.12(2)$ . Lower Plot: Correlation length for a fixed system size of  $L = 100$  [see equation (7) for a definition of  $\xi$ ], as we move through the critical line and a disorder point at  $\alpha_d(\beta = 0.2) = 0.100(5)$ .

cally *decrease* to that of the TB point under the RG flow (along the thick black flow line in Fig. 3). This latter constraint means that the central charge must be larger than  $c_0 = 3/2$  of the  $SU(2)_2$  theory.

We show in the Section VIII B that the simplest conformal field theory that satisfies these requirements is the  $SU(2)_{k=4}$  WZW theory. The Lie group  $SU(2)$  is natural because the Hamiltonian is generically  $SU(2)$ -symmetric (higher “accidental” symmetry is possible, but would require fine-tuning the parameters of the Hamiltonian). As for the level  $k = 4$ , we give a formal argument based on conformal embedding in Sect. VIII B, but this can be understood qualitatively as follows. The Hamiltonian in Eq. (1) can be represented as two  $S = 1$  spin chains, each with half as many sites, interacting via the intra-chain coupling  $J_2 = \alpha J_1$ , see Fig. 6. The two chains are coupled by the Heisenberg as well as biquadratic spin-spin interaction, so that the Hamiltonian  $H = H_0 + H_\perp$ :

$$H_0 = J_2 \sum_{\alpha=1}^2 \sum_i \mathbf{S}_{\alpha,i} \cdot \mathbf{S}_{\alpha,i+1} \quad (3)$$

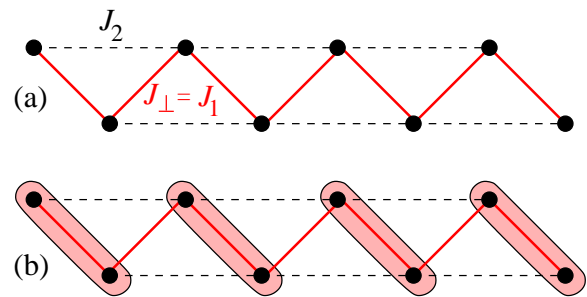


FIG. 6: (Color online) Schematic representation of two coupled  $S = 1$  spin chains. (a) The spin coupling within each chain is given by the interaction  $J_2 = \alpha J_1$  in the original model Eq. (1). (b) The dimerized ground state, with the circled rungs corresponding to the spin singlet or triplet of two spins, depending on the sign of the interchain coupling  $J_\perp = J_1$ .

$$H_\perp = J_\perp \sum_i \sum_{\delta=\pm 1/2} \mathbf{S}_{1,i+1} \cdot \mathbf{S}_{2,i+\delta} + \beta (\mathbf{S}_{1,i+1} \cdot \mathbf{S}_{2,i+\delta})^2,$$

where  $J_\perp = J_1$  in the original model Eq. (1). In the limit  $J_2 \gg J_1$  ( $\alpha \gg 1$ ), the two chains are decoupled and each can be described by the perturbed WZW theory in Eq. (2). However for finite  $J_1$ , the local staggered magnetizations of the two chains can lock together, forming a combined spin  $S = 2$  object. This is particularly evident in the case of a ferromagnetic coupling  $J_1$ , when the two chains form a ladder of triplets, leading to a dimerized ground state shown in Fig. 6b. For antiferromagnetic interchain coupling  $J_1$ , the situation is similar but it is the singlets that form instead on the dimerized bonds. The bottom line is that emergent  $S = 2$  excitations can form. Provided these excitations are gapless at a (multi)critical point, it was proposed by Affleck<sup>52</sup> that they are described by  $SU(2)_k$  WZW conformal field theory at level  $k = 2S$ . This has been corroborated recently by numerical calculations<sup>53</sup>. In our case  $S = 2$  and the resulting theory is thus  $SU(2)_4$ .

The  $SU(2)_4$  WZW theory has central charge  $c = 2$  and the RG flow towards the TB point (Fig. 3) indeed satisfies Zamolodchikov’s “ $c$ -theorem”<sup>49</sup> mentioned earlier. The analysis shows that the theory has 4 primary fields, however only two of them satisfy the symmetries of the Hamiltonian and are therefore allowed as perturbations<sup>54,55</sup>. These two primary fields have conformal dimensions  $(\frac{1}{3}, \frac{1}{3})$  and  $(1, 1)$ . The corresponding field bilinears have scaling dimensions  $\Delta_1 = 2/3$  (relevant) and  $\Delta_2 = 2$  (marginally relevant). In addition, the current bilinear  $\bar{J}^a J^a$  (scaling dimension  $\Delta_3 = 2$ ) is also allowed, however it is marginally irrelevant and leads only to logarithmic corrections to scaling. As per our requirement, the  $SU(2)_2$  theory thus possesses two relevant fields, making  $\Omega$  an unstable fixed point. The field with dimension  $\Delta_1 = 2/3$  plays a role similar to the mass term in Eq. 2, resulting in a transition into the Haldane phase or the dimer phase, depending on the sign of the coupling constant. The other (marginally) relevant field, with di-

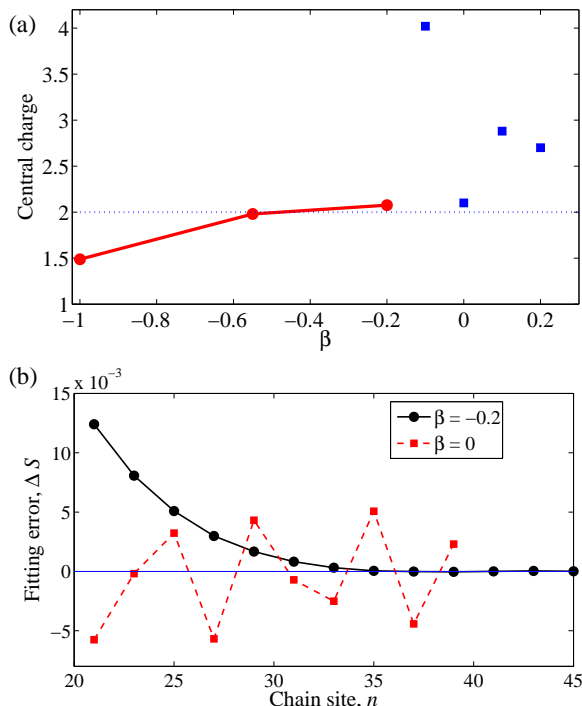


FIG. 7: (Color online) (a) Central charge  $c$  for different values of  $\beta$  along the critical line in Fig. 3, extracted by fitting the DMRG entanglement entropy to Eq. (4). The red circles mark the values of  $c$  determined reliably, and the blue squares denote the data points where conformal scaling does not apply, as illustrated by (b): the error of fitting DMRG data to Eq. (4) for  $\beta = -0.2$  and  $\beta = 0$ .

mension  $\Delta_2 = 2$ , governs the transition into the gapped NNN-AKLT phase (purple flow line in Fig. 3).

Note that the central charge  $c = 2$  suggests that the  $SU(2)_4$  theory can be recast in the form of the 2 copies of bosonic fields. This is indeed possible<sup>54</sup>, however these bosonic fields are highly non-local, explaining the non-trivial fractional scaling dimensions of the primary fields.

### 3. Numerical results for the central charge

To verify the field-theoretical predictions, we have extracted the central charge from our DMRG calculations of the entanglement entropy, known to scale in an open 1D system as follows<sup>56,57</sup>:

$$S(n) = S_0 + \frac{c}{6} \ln \left[ \frac{2L}{\pi} \sin \left( \frac{\pi n}{L} \right) \right], \quad (4)$$

where  $n$  is the site number in the chain of length  $L$  marking the end of a contiguous block of  $n$  sites for which the entanglement entropy is calculated. The central charge  $c$  determined in this way is plotted in Fig. 7a for different values of  $(\beta_c, \alpha_c)$  along the critical line in Fig. 3. As mentioned earlier, the critical line is terminated at the critical end-point  $\Omega = (\beta^*, \alpha^*)$ . We find that the entanglement entropy follows the scaling in Eq. (4) for values

of  $-1 \leq \beta_c < \beta^*$  and fails for larger values of  $\beta_c$ , as evident from the fitting error in Fig. 7b. This failure occurs because the system is no longer critical for  $\beta_c > \beta^*$  and has a finite spectral gap, so the blue data points in Fig. 7a no longer have a meaning of a central charge. From this, as well as from the DMRG calculation of the spectral gap, we were able to put brackets on the value of  $\beta^*$  to lie in the interval  $-0.2 < \beta^* < -0.15$ , with the corresponding bracket on  $\alpha^*$  within  $0.47 < \alpha^* < 0.53$ .

To summarize, we have demonstrated that the phase diagram of the spin-1 chain, shown schematically in Fig. 3, is characterized by a continuous transition from the Haldane to the dimer phase for  $-1 \leq \beta < \beta^* \approx -0.2$ , with vanishing spectral gap and divergent correlation length along the critical line (see Fig. 4). For larger  $\beta$ , the transition becomes first-order, with the spectral gap remaining open as  $\alpha$  increases (see Fig. 5), in agreement with previous DMRG<sup>11,12</sup> and field-theoretical studies<sup>13</sup> at  $\beta = 0$ . We conjecture that separating these two regimes is a multi-critical end-point at  $\Omega = (\beta^*, \alpha^*)$ , which terminates the line of second-order phase transitions. Everywhere to the left of this point, the RG flow along the critical line is governed by the marginally irrelevant perturbation to the  $SU(2)_2$  WZW theory. However the point  $\Omega$  itself lies in a different universality class of the  $SU(2)_4$  Wess-Zumino-Witten theory. The field-theoretical analysis is corroborated by the DMRG calculation of the central charge, which agrees very well with the conformal field theory predictions.

## B. Edge Excitations

We now consider the nature of the ground state wave function as we move across the critical line. As mentioned in the introduction, the Haldane phase (also referred to as AKLT phase) possesses effectively free  $S = 1/2$  spins on the edges with zero-energy edge excitations, which give rise to the four-fold degenerate ground state for a finite chain with open boundary conditions. As has been realized early on, the existence of these edge excitations is a hallmark of the topological nature of the Haldane phase. By contrast, the dimer phase is not topological and lacks edge excitations<sup>16,21</sup>. The nature of the ground state wave function can thus be characterized by the existence or absence of edge excitations.

Using the DMRG we are able to probe the edge excitations directly, by considering the magnetization  $\langle S^z(x) \rangle$  along the chain. Edge excitations show up clearly in the Haldane phase in the form of a large magnetization confined to the chain ends<sup>12</sup>, as shown in Fig. 8. Another way to probe the existence of the edge excitations in DMRG is by measuring a spectral gap between projections onto different total spin  $S_{tot}^z$  sectors. In the Haldane (AKLT) phase, the  $S_{tot} = 0$  ground state is degenerate with the first excited triplet in the  $S_{tot} = 1$  sector (the so-called ‘‘Kennedy triplet’’<sup>17</sup>), resulting in the aforementioned four-fold degenerate ground state in

an open chain, which is the consequence of the so-called  $Z_2 \times Z_2$  spontaneous symmetry breaking<sup>16</sup>. The lowest true bulk excitation lies in the  $S_{tot} = 2$  sector<sup>11,12</sup>, and therefore, the bulk Haldane gap  $\Delta$  is determined by the difference of the ground state energy in the symmetry sectors  $S_{tot} = 0$  and  $S_{tot} = 2$ , and is plotted in Figures 4 and 5. By contrast, the gap to edge excitations  $\Delta_{edge}$ , which we emphasize is *not* the true bulk gap, is the difference of the ground state energies between the symmetry sectors  $S_{tot} = 0$  and 1. Therefore, the signature of the Haldane phase is the vanishing gap to edge excitations  $\Delta_{edge} = 0$ .

Upon the transition to the translational-symmetry breaking dimer (NNN-AKLT) phase for  $\alpha > \alpha_c(\alpha_T)$  the edge excitations become gapped out. This is clearly seen in the gap  $\Delta_{edge}$ , at a fixed system size shown in Figures 8a,b for both negative and positive  $\beta$ . In addition, this transition manifests itself in the character of edge excitations, which we extract by plotting the magnetization along the chain in the ground state symmetry sector  $M(x)|_{S_{tot}=0} = \langle S^z(x) \rangle$ . On approaching the critical line from the AKLT phase below, the edge excitations bleed into the bulk of the chain, as shown clearly in figure 8c. We therefore conclude that the nature of the ground state wave function changes from topologically non-trivial inside the AKLT phase to topologically trivial in the TSBP phase above the critical line.

#### IV. PHASES

We now proceed to determine the topology of the phase diagram shown schematically in figure 2. By using a combination of the DMRG and a MPS variational wave function we are able to identify and describe the nature of each phase as well as the character of the ground state wave function.

##### A. Haldane Phase

Fixing the value of  $\beta$  and tuning  $\alpha$  we find the Haldane phase (originally defined in the range  $-1 < \beta < 1$  for  $\alpha = 0$ ) now extends over a region of finite  $(\beta, \alpha)$  as shown in the schematic phase diagram and the quantitative phase diagram in figure 20. The Haldane phase is gapped and characterized by short range antiferromagnetic correlations. The spin-spin correlation function is well described the Ornstein-Zernicke (OZ) form in two dimensions (see equation 7 and section V for discussion). The AKLT phase also posses a doubly degenerate ground state and resulting gapless edge excitations. Lastly, the AKLT phase is known to break a hidden  $Z_2 \times Z_2$  symmetry and as a consequence the string order parameter is finite<sup>29</sup>.

We find the ground state wave function can be qualitatively described by the AKLT wave function ansatz which yields a ground state energy  $E_{AKLT}(\alpha, \beta) = -4/3 +$

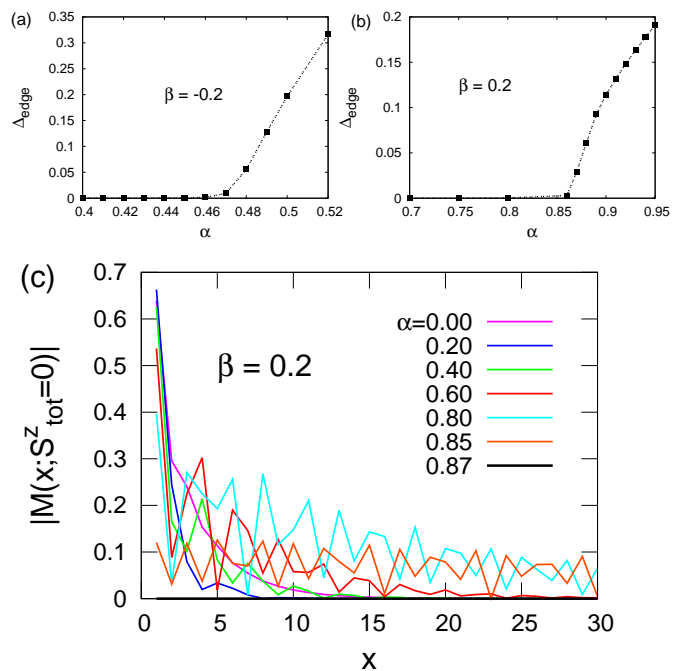


FIG. 8: (Color online) The gap to edge excitations  $\Delta_{edge}$  at a fixed system size  $L$ , opening up as  $\alpha$  crosses the critical line from the AKLT phase at  $\alpha_c(\beta = -0.2) = 0.480(5)$ ,  $L = 80$  (a) and  $\alpha_T(\beta = 0.2) = 0.855(5)$ ,  $L = 100$  (b). We clearly see the edge excitations become gapped out. (c) The absolute value of magnetization along the chain in the  $S_{tot} = 0$  symmetry sector approaching the critical line from the AKLT phase for  $\beta = 0.2$ . We see the edge excitations begin to bleed into the bulk of the chain as the correlation length increases and then vanish as we cross the transition line at  $\alpha_T(\beta = 0.2) = 0.855(5)$ .

$4\alpha/9 + 2\beta$ . When compared to DMRG calculations, the naive estimate does quite a good job, while the variational estimate is more accurate, see figures 11b and 12b. We note that the AKLT wave function ansatz is almost exact along the disorder line and we will return to this point in detail in section VB. We also find the double degenerate ground state survives up to the critical line as shown in figures 8. Lastly, we have not calculated the string order parameter but due to the presence of edge states we expect it to remain finite over the entire Haldane phase.

##### B. Spontaneously Dimerized Phase

We now come to the dimerized phase. In order to characterize the amount of dimerization we find it useful to define the dimer order parameter

$$D(\alpha, \beta) = \frac{1}{N_D} \sum_{i=1}^{N_D} (-1)^i \langle \mathbf{S}_{i+1} \cdot \mathbf{S}_{i+2} - \mathbf{S}_i \cdot \mathbf{S}_{i+1} \rangle, \quad (5)$$

where  $N_D = L - 2$  serves as a normalization. We find the dimer order parameter rises continuously from zero

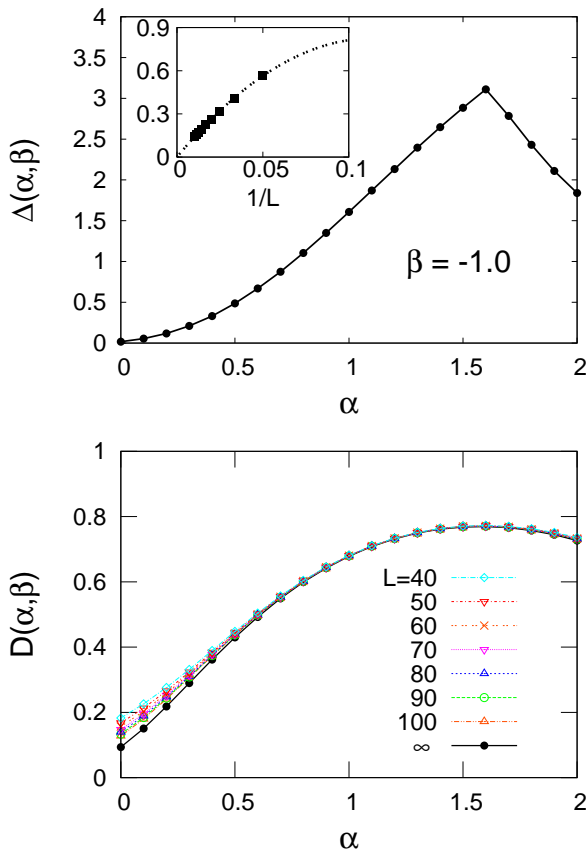


FIG. 9: (Color online) Upper Plot: The bulk gap  $\Delta$  between symmetry sectors  $S_{tot} = 0$  and 2 for fixed  $\beta = -1$  tuning away from the TB point. We see the gap opens continuously for a finite value of  $\alpha$ . Inset: Extrapolating the gap at the TB point ( $\beta = -1.0$  and  $\alpha = 0$ ) to the thermodynamic limit, the fit is in excellent agreement with a gapless point namely,  $\Delta(L) = a_{\Delta}/L + b_{\Delta}/L^2$ . When fit to a functional form for a finite gap [see equation (10)] we find a small gap at the TB equal to 0.017(2). Lower Plot: Dimer order parameter, defined in equation 5 as a function of the system size  $L$  and extrapolated to the thermodynamic limit, clearly displaying the system enters the dimer phase immediately upon tuning  $\alpha$  away from the TB point. The finite value of  $D(\alpha = 0, \beta = -1)$  at the TB point is attributed to not reaching large enough system sizes at the critical point.

on entry into the dimer phase. The dimerized phase is gapped with a ground state wave function well described by the dimerized wave function ansatz (see section VIII) as shown in figure 11b. We show in section V the spin-spin correlation function is well described by a dimerized OZ form (see equation 9). Lastly, we find the edge excitations are gapped on entry into the dimerized phase (see figure 8) with a diverging correlation length (on the order of the system size).

In order to determine the topology of the dimerized phase we first consider tuning away from the TB point with a finite  $\alpha$ , (i.e. fixing  $\beta = -1$ ). With the DMRG at the TB point we find a ground state energy  $E_{GS} =$

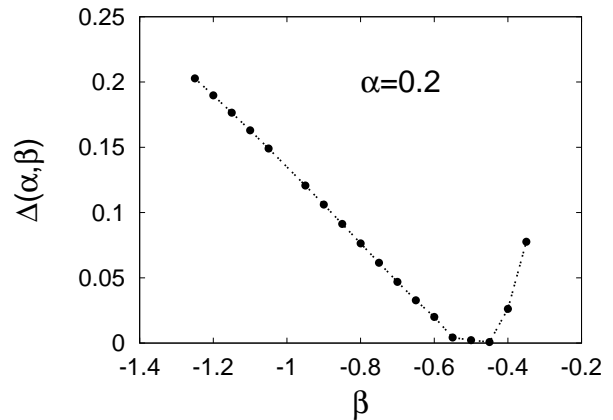


FIG. 10: Bulk gap  $\Delta$  in the vicinity of the TB point for a fixed NNN coupling  $\alpha = 0.2$ , as a function of  $\beta$ . From the behavior of the gap, it is clear the critical line will move towards a smaller value of  $\beta$ , as we increase  $\alpha$  away from the TB point, verifying the slope of  $\alpha_c(\beta)$  shown in the schematic phase diagram 2.

–3.999 in agreement with the exact Bethe ansatz result<sup>22,23</sup> of –4.0. In addition, as previously discussed the TB point has a central charge of  $c = 1.5$  while we obtain 1.49 with the DMRG. Within numerical accuracy we find a finite value of  $\alpha$  continuously opens the bulk gap  $\Delta(\alpha, \beta)$ , see figure 9. In addition, we find the dimer order parameter rises continuously tuning away from the TB point, clearly marking the entry into the dimer phase. We remark that in the vicinity of the TB point, the diverging correlation length makes the identification of the critical line quite challenging without going to much larger chain sizes than we have in the present study.

In order to determine the slope of the critical line starting from the TB point we consider fixing the NNN coupling  $\alpha = 0.2$  and varying  $\beta$  to determine if the transition moves to either a larger or smaller value of  $\beta$ . By calculating the gap, shown in figure 10, it is quite clear the critical line moves towards a smaller value of  $\beta$  verifying the slope of  $\alpha_c(\beta)$  shown in the schematic phase diagram 2. In addition, we find a small gap [ $\Delta(\alpha = 0.2, \beta = -0.5) = 0.0022$ ] at the critical point  $\beta_c(\alpha = 0.2) \approx -0.50(5)$ , and a central charge of  $c = 1.98$  as discussed previously in section III A. Interestingly, as shown in figure 10 for  $\beta < \beta_c$  we find  $\Delta(\alpha, \beta) \propto \beta_c(\alpha) - \beta$ , similar to the vicinity of the TB point.

We now consider a range of parameters by fixing  $\beta$  in the range  $-1.0 < \beta \leq -0.2$  and tuning  $\alpha$ . In the following, we present results for  $\beta = -0.2$  which we find to be close to the proposed multi-critical point  $\Omega$ . The dimer order parameter in the thermodynamic limit (see figure 11a) rises continuously out of the AKLT phase and then decreases on entering the NNN AKLT region of the phase diagram. We find the ground state energy agrees very well with the result from the dimerized wave function ansatz which yields an  $\alpha$  independent ground state energy  $E_{Dimer}(\alpha, \beta) = 8\beta/3 - 1$ . In addition, with the

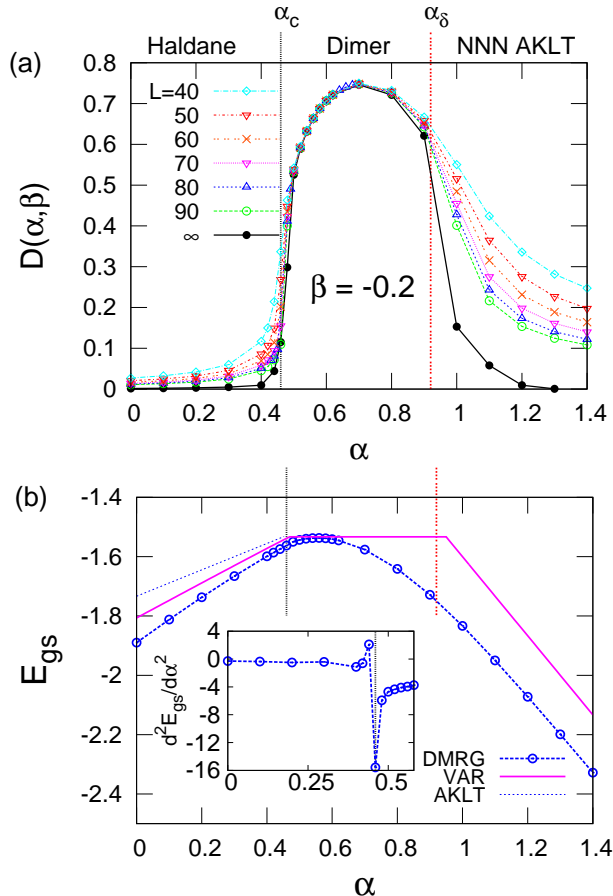


FIG. 11: (Color online) (a) The dimer order parameter  $D(\alpha, \beta)$  as a function of  $\alpha$  for  $\beta = -0.2$  for various system sizes  $L$ . In the dimer phase we find the order parameter is independent of system size implying  $D(\alpha, \beta)$  is finite in the thermodynamic limit, whereas deep inside the NNN AKLT phase ( $\alpha \gtrsim 1.2$ ), we find that  $D(\alpha, \beta)$  does not saturate in  $L$  and likely becomes vanishingly small in the thermodynamic limit. (b) The ground state energy as a function of  $\alpha$  for  $\beta = -0.2$  obtained within DMRG (circles) compared to the AKLT, NNN AKLT, dimer, and variational wave functions. Note, the naive estimate of the ground state energy of the dimer and NNN AKLT wave functions agrees with the variational result and is therefore not shown. We have clearly marked the critical line  $\alpha_c$  as well as the cross over line  $\alpha_\delta$  from the dimer to the NNN AKLT phase (see section V C 2 for a definition of  $\alpha_\delta$ ). Inset: The numerical second derivative of the ground state energy as a function of  $\alpha$ , we find a discontinuity in  $d^2 E_{gs}/d\alpha^2$  at the critical point, which suggests the transition into the dimer phase is second order.

DMRG, we find a discontinuous second derivative of the ground state energy as we cross the critical line (see figure 11b). We note, this implies the phase transition is second order and is consistent with the field theoretical discussion, the very small gap, and the diverging correlation length at the transition (see figure 4).

Interestingly, in the vicinity of  $-0.2 < \beta < -0.15$  and  $0.47 < \alpha < 0.53$  we find the critical and disorder lines intersect (see section V for a discussion of disorder points). This has serious physical implications, at the disorder

point the correlation length goes through a *minimum*, which implies at this point it is not possible for the correlation length to diverge. Therefore, consistent with the field theoretical results, we find the critical line terminates into a line of first order transitions at the point  $\Omega$  which lies in the area  $(-0.2, 0.47) < \Omega < (-0.15, 0.53)$ . For  $\beta = -0.175$  the correlation length at the transition is only moderately enhanced on the order of  $\xi(\alpha, \beta) = 10.0$  (in units of the lattice spacing) and the edge excitations vanish. For the case of  $\beta = -0.15$  the close vicinity to the disorder line makes the identification of  $\alpha_T(\beta)$  difficult, since at the disorder point the correlation length experiences a minimum. Here, we track the transition via the suppression of edge excitations and we find the result  $\alpha_T(\beta = -0.15) = 0.530(5)$  which actually agrees well with the wave function approaches, see Fig. 13.

### C. NNN AKLT

The NNN AKLT phase<sup>11,12</sup> is gapped with incommensurate spin-spin correlations in both real and momentum space (see section V for a detailed discussion). The dimer order parameter is not a suitable variable to describe the short range incommensurate correlations and is therefore vanishingly small (in the thermodynamic limit) across the NNN AKLT phase as shown in figures 11a, 12a. In addition, for a finite  $\alpha$  in the NNN AKLT phase the edge excitations are gapped out, whereas for an infinite  $\alpha$  there are effectively two copies of spin-1 chains and are therefore the ground state is 16 fold degenerate, coming from two spin-1/2s on each end of the chain<sup>11,12</sup>. However, any finite  $J_1$  is enough to couple the edge spins of the two chains, which form singlets and are gapped out. Interestingly, we find the NNN AKLT phase exists over a finite range of  $(\beta, \alpha)$  provided  $\alpha$  is large enough. In particular, we consider fixing  $\beta$  in the range  $[-0.125, 0.4]$  and tuning  $\alpha$  as shown in the quantitative phase diagram in figure 20. In addition, we find the ground state wave function is well described by the NNN AKLT wave function ansatz (see section VIII). This is shown in figures 11b and 12b, where the ground state energy acquires the same slope as the naive NNN AKLT wave function ansatz  $E_{NNN}(\alpha, \beta) = 4/3(\beta - \alpha)$ . Since we have not calculated the string order parameter, we use the vanishing edge states to locate the transition line into the NNN AKLT phase. In addition, we track the entry into the NNN AKLT phase by a maximum in the spin-spin correlation length and the gap passing through a minimum. We therefore conclude  $\alpha_T(\beta)$  has the same properties as  $\alpha_T(\beta = 0)$ .

### D. Variational Phase Diagram

Using a variational wave function constructed out of Matrix Product States (MPS) we interpolate between the AKLT, dimer and NNN AKLT wave functions. The

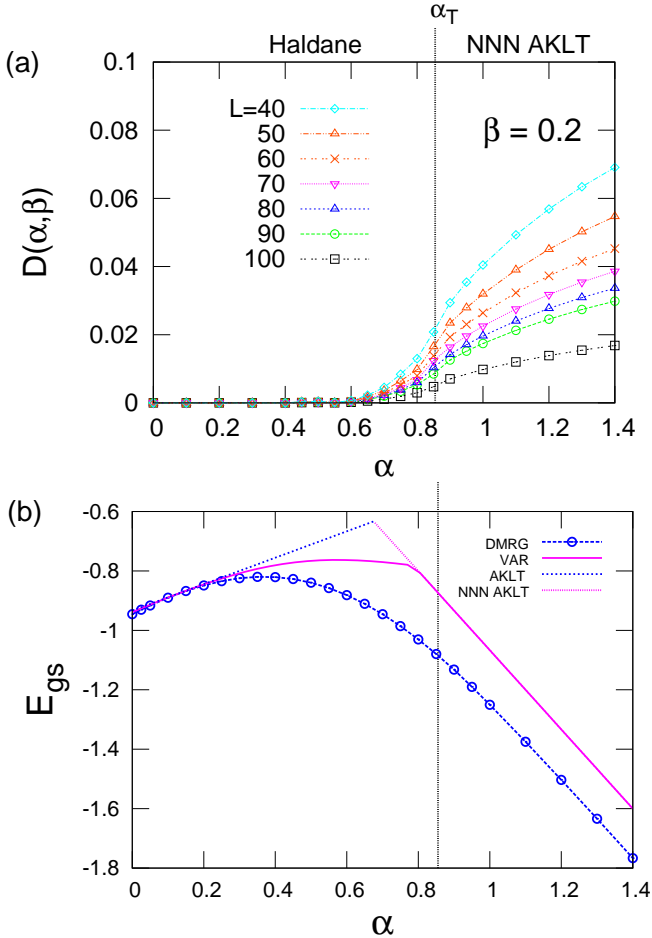


FIG. 12: (Color online) (a) The dimer order parameter  $D(\alpha, \beta)$  as a function of  $\alpha$  for  $\beta = 0.2$  for various system sizes  $L$ . The dimer order parameter is identically zero in the Haldane phase, whereas inside the NNN AKLT phase, we find that  $D(\alpha, \beta)$  does not saturate in  $L$  and may become vanishingly small in the thermodynamic limit. (b) Comparison of the ground state energy for  $\beta = 0.2$  as a function of  $\alpha$  between the DMRG results (circles), the AKLT ansatz (dashed line) and the variational wave function (continuous line). For large values of  $\alpha$  the ground state energy approaches the NNN AKLT ansatz. The first order transition shows up clearly in both the AKLT and variational solutions, but the first numerical derivative of the ground state energy obtained within DMRG show no sign of a discontinuity at  $\alpha_T$ , consistent with references [11,12].

details of the method are described in section VIII. By considering the ground state energy we can find the location of a critical line within the variational approach and the phase diagram is presented in figure 13. We find the critical line within the MPS formalism is a line of first order transitions separating the Haldane phase and both the dimer and the NNN AKLT phases. Moreover, within the MPS formalism, the (true) crossover between the dimer and the NNN-AKLT phases is spuriously resolved as a first order phase transition. This is clearly an artifact of the variational treatment, since the DMRG calculations verify the existence of a cross over.

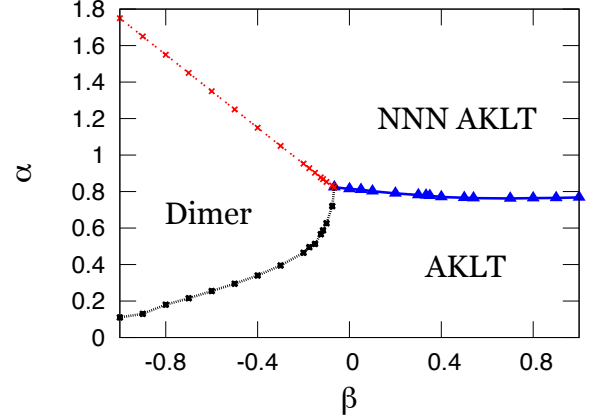


FIG. 13: (Color online) Phase diagram obtained using the MPS variational treatment, with each phase described in the text. A line of first order transitions (blue triangles) separates the Haldane phase from its two adjacent phases, on the left the dimer phase (separated by black crosses), and the NNN-AKLT phase above. The red x's represent the cross over line (falsely identified as a transition within the variational treatment) to the NNN AKLT phase, and the absence of dimerization.

The variational treatment interpolates between the three trial wave functions corresponding to the AKLT, NNN-AKLT, and dimer ground states, and indicates first order phase transitions between these three phases. While there is indeed a such a phase transition between the NNN-AKLT and AKLT phases, as we have stated in the previous sections, the remainder of the phase diagram is more nuanced than such a naive MPS approach can capture. Despite its shortcomings, the phase diagram agrees qualitatively with the phase diagram calculated by DMRG (see Fig. 20). Moreover, in the approach to  $\beta = 0$  from the left, the agreement is even quantitatively reasonable. Note however, that the variational approach underestimates  $\alpha_T$  the transition point between AKLT and NNN-AKLT as a function of  $\beta$  for  $\beta > 0$ , and predicts an incorrect trend for  $\alpha_T(\beta)$  (compare Fig. 20).

## V. SHORT RANGE ORDER

### A. Introduction to Disorder and Lifshitz Points

As mentioned in the introduction, Haldane's mapping<sup>10</sup> to the two dimensional non-linear sigma model implies the antiferromagnetic quantum spin chain can be regarded as a two dimensional classical spin model at a temperature  $T_{\text{eff}} \propto 1/S$ . As a consequence of the Mermin Wagner theorem<sup>43</sup> it is well known that for sufficiently short range interactions, the classical two dimensional Heisenberg model cannot break a continuous

symmetry at finite temperature and therefore will not order. Therefore, as a result of the mapping, the nearest neighbor Heisenberg quantum spin chain can not exhibit long range magnetic order. However, it is possible to break a discrete symmetry in two dimension, as we have shown and discussed in the previous sections. Also, in the context of two dimensional classical spin models discrete symmetries can be broken tuning anisotropies and different types of frustration.

Without breaking any symmetry, it is possible for quantum spin chains to possess short range order (as discussed in the introduction). It has been shown tuning either the biquadratic<sup>29</sup> or next nearest neighbor interaction<sup>11,12</sup> can introduce short range incommensurate order that can be characterized as a disorder point or Lifshitz point, where the incommensurate correlations appear in either real or momentum space respectively.

Disorder points of the first kind and Lifshitz points have been well defined in classical statistical mechanics and have been discussed extensively in the context of quantum spin chains in<sup>11,12,29</sup> (and references there in) therefore we briefly review the concepts here. There are two types of disorder points<sup>29</sup>, in the following manuscript we will only encounter a disorder point of the first kind so for the following we will refer to it as a disorder point. Tuning the control parameter  $\lambda$  of a Hamiltonian across the phase diagram, the system will pass through a disorder point at  $\lambda_d$  if the correlation length  $\xi_A(\lambda)$  [where  $A$  denotes the commensurate ( $C$ ) and incommensurate ( $IC$ ) phase] develops an infinite slope on the commensurate side but is generally finite on the incommensurate side, i.e.  $d\xi_C(\lambda_d)/d\lambda = \infty$  and  $d\xi_{IC}(\lambda_d)/d\lambda < \infty$ . In addition, the wave number of the correlation function  $q_A(\lambda)$  changes from a commensurate to an incommensurate value at  $\lambda_d$ . In the commensurate phase  $q_C(\lambda < \lambda_d)$  is constant and as a result of the disorder point it develops an infinite slope on the incommensurate side, i.e.  $dq_C(\lambda_d)/d\lambda = 0$  and  $dq_{IC}(\lambda_d)/d\lambda = \infty$ .

In the vicinity of  $\lambda_d$  on the incommensurate side the wave number rises continuously

$$q_{IC}(\lambda) - q_C(\lambda_d) \propto (\lambda - \lambda_d)^\sigma, \quad (6)$$

with a non-universal exponent  $\sigma$ . The generic behavior of  $\xi$  and  $q$  across a disorder point are shown in figures 14 (a) and (b). Interestingly, these features have been found across numerous different physical scenarios in both classical and quantum models. Upon further tuning  $\lambda$  the system will pass through a Lifshitz point at  $\lambda_L$  where the correlation function in momentum space goes from a single commensurate peak to a two peak incommensurate structure.

For systems in a broken symmetry state, the disorder and Lifshitz points merge into a single line and separate the commensurate and incommensurate phases, in two dimensions this will remain a cross over. In the disordered phase, the disorder and Lifshitz lines split into two different cross over lines, this is shown schematically in

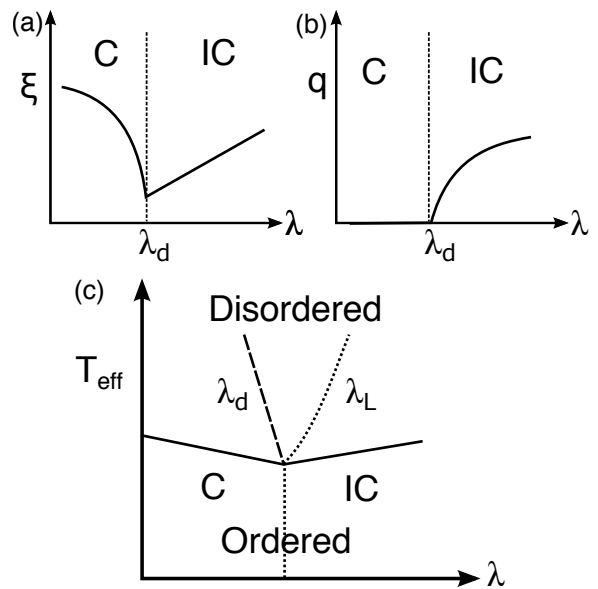


FIG. 14: Schematic figures displaying a disorder point in the correlation length  $\xi$  (a) and the wave number  $q$  (b).  $C$  and  $IC$  denote commensurate and incommensurate correlations in real space. Generic phase diagram of breaking a discrete symmetry via tuning an effective energy scale  $T_{\text{eff}}$  in two dimensions in the presence of incommensurate correlations  $\lambda$  (c).

figure 14 (c). We would like to point out the remarkable similarities between our results in figures 2 and 20, and the generic phase diagram in figure 14 (c), where we see on the symmetry broken side the disorder and Lifshitz lines have merged into one, whereas on the disordered side they have split into two.

## B. Results: $0 < \beta < 1$

In the following section, we show by fixing  $\beta > 0$  and varying  $\alpha$  that the model defined in equation (1) passes through a disorder point and a Lifshitz point. This allows us to conclude there is a line of disorder and Lifshitz points in the  $\beta - \alpha$  phase diagram.

### 1. Short Range Order: Disorder and Lifshitz lines

Guided by the mapping to a two dimensional classical spin model as well as previous studies in the spin-1 Heisenberg chain<sup>11,12,29,37</sup> we expect the real space correlation function  $C(x) = \langle \mathbf{S}(x) \cdot \mathbf{S}(0) \rangle$  to obey the two dimensional Ornstein-Zernicke form

$$C_{OZ}(x) \propto \cos[q(\alpha, \beta)x] \frac{e^{-x/\xi(\alpha, \beta)}}{\sqrt{x}}, \quad (7)$$

we extract both the correlation length  $\xi(\alpha, \beta)$  and the wave number  $q(\alpha, \beta)$  from fitting our numerical data to

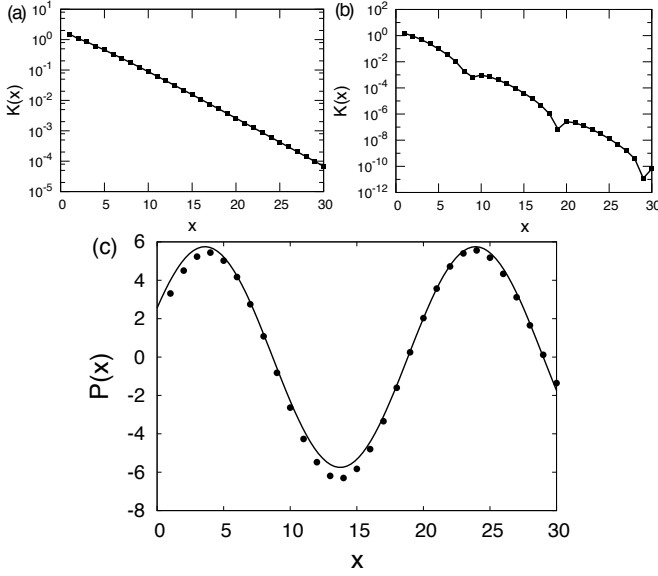


FIG. 15: The real space correlation function  $C(x)$ , plotted in terms of  $K(x) \equiv C(x)(-1)^x \sqrt{x}$  to extract the correlation length  $\xi(\alpha, \beta)$  for  $\beta = 0.1$  on either side of the disorder point at  $\alpha_d(\beta = 0.1) = 0.180(2)$  with  $\alpha = 0.1 < \alpha_d(\beta)$  (a) and  $\alpha = 0.2 > \alpha_d(\beta)$  (b). Note the presence of incommensurate real space correlations in (b) in the form of peaks. Extracting the wave number  $q(\alpha, \beta)$  by plotting  $C(x)$  in terms of  $P(x) \equiv K(x) \exp(x/\xi)$  for  $\beta = 0.1$  and  $\alpha = 0.2$ , the numerical data are circles and the solid line is a fit to the data (c).

equation (7). Fixing  $\beta = 0.05, 0.10, 0.20, 0.30$ , such that we have not passed through the disorder point at  $\beta = 1/3$  for  $\alpha = 0$  (which occurs at the AKLT point<sup>18,29</sup>) and the real space correlations are commensurate with a wave vector  $q(\alpha < \alpha_d(\beta), \beta) = \pi$  we then tune  $\alpha > 0$  passing through a disorder point at  $\alpha_d(\beta)$ .

To extract the correlation length we fit the numerical data to  $K(x) \equiv C(x)(-1)^x \sqrt{x}$ , using a similar procedure as described in reference<sup>29</sup>, namely, for  $\alpha < \alpha_d(\beta)$  we can directly fit our data to the functional form  $K(x)$ , where for  $\alpha > \alpha_d(\beta)$  we fit the maxima to the function  $K(x)$ . We extract the wave number by fitting the data to the functional form  $P(x) \equiv K(x) \exp(x/\xi)$ , see figure 15. Our results allow us to conclude, the real space correlation function in this region of the phase diagram is well described by the two-dimensional Ornstein-Zernicke form in equation (7).

In figure 16 we present the correlation length  $\xi(\alpha, \beta)$ , for various values of  $\alpha$  and  $\beta$ , we find  $\xi(\alpha, \beta)$  experiences a minimum at  $\alpha_d(\beta)$  with a large slope for  $\alpha < \alpha_d(\beta)$ . In addition, over the same set of  $\alpha$  and  $\beta$  we find the wave number  $q(\alpha, \beta)$  rises continuously from  $\pi$  for  $\alpha > \alpha_d(\beta)$ , see figure 16. In the vicinity of  $\alpha_d(\beta)$ , we have found the exponent  $\sigma(\alpha, \beta)$  defined in equation (6) [with  $\lambda$  replaced by  $\alpha$  and  $\lambda_d$  replaced with  $\alpha_d(\beta)$ ], in each case satisfies  $0 < \sigma(\alpha, \beta) < 1$  consistent with  $q(\alpha, \beta)$  having an infinite slope on the incommensurate side. These results allow us to conclude that each  $\alpha_d(\beta)$  is in fact a disorder point

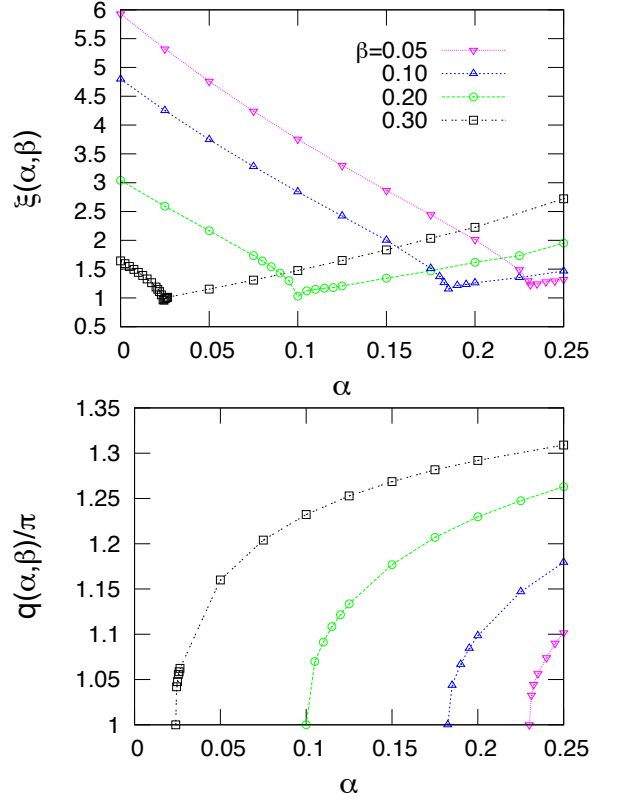


FIG. 16: (Color online) Upper Plot: The correlation length  $\xi(\alpha, \beta)$  for various values of  $\alpha$  and  $\beta$ . We identify the minimum in  $\xi(\alpha, \beta)$  as a disorder point. Note that the value of the correlation length at the disorder point is increasing as  $\beta$  decreases. Lower plot: The wave number  $q(\alpha, \beta)$  as a function of  $\alpha$ . We find  $q(\alpha, \beta)$  rises continuously from  $\pi$  at  $\alpha_d(\beta)$  to an incommensurate value.

which defines a line of disorder points in the  $\beta - \alpha$  phase diagram, see figures 2 and 20. Our results imply the AKLT point in the biquadratic chain ( $\alpha = 0$ ) is smoothly connect to the disorder point in the next nearest neighbor chain ( $\beta = 0$ ) in the  $\beta - \alpha$  phase diagram.

Directly at each disorder point  $\alpha_d(\beta)$  our results can be fit equally well with a purely exponential decay as well as the functional form in equation (7). As a result it is quite challenging to determine the functional form of the correlation function  $C(x)$  directly at the disorder point with numerics alone. We would like to point out that disorder points are expected to be accompanied with a dimensional reduction, in our case  $C(x)$  would obey the one dimensional Ornstein-Zernicke form, i.e. purely exponential decay, this is the case at the VBS point where the identification is possible due to the exact solution<sup>18,29</sup>. However, we can still gain insight by using the AKLT wave function to track how close the DRMG ground state is to the AKLT ansatz. We find the region between disorder and Lifshitz lines, namely  $\alpha_d(\beta) < \alpha(\beta) < \alpha_L(\beta)$  is closest to the AKLT ground state. Physically, the disorder point marks the entry into the AKLT ground state region for a finite  $\alpha$ , see figure 17.

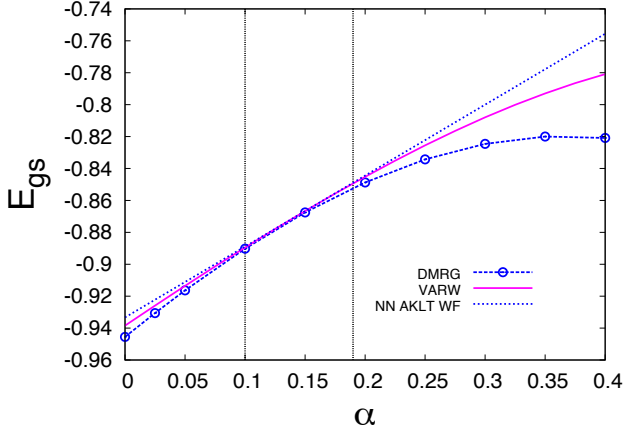


FIG. 17: (Color online) Comparison of the ground state energy for  $\beta = 0.2$  as a function of  $\alpha$  between the DMRG results (points), the AKLT ansatz (dashed line) and the variational wave function (continuous line). Zoomed in region around the disorder and Lifshitz points (dashed lines), upon crossing the disorder point the ground state is very close to the AKLT ansatz.

We now turn to the correlation function in momentum space

$$S(q) = \sum_x e^{iqx} C(x). \quad (8)$$

We consider  $\beta = 0.05, 0.10, 0.20, 0.30, 0.35, 0.40$ , such that the model for  $\alpha = 0$  has not passed through the Lifshitz point at  $\beta_L(\alpha = 0) = 0.43806(4)$  (Ref. 39). Tuning  $\alpha > 0$  we find a line of Lifshitz points at  $\alpha_L(\beta) > \alpha_d(\beta)$  as the peak in  $S(q)$  at  $q = \pi$  softens into an incommensurate double peak structure (see figure 18) which saturates at  $q = \pm\pi/2$  as the a result of the doubling of the lattice spacing for large values of  $\alpha$ . As a consequence of the Lifshitz point, for values of  $\alpha > \alpha_L(\beta)$  the excitation spectrum develops a double degenerate structure.

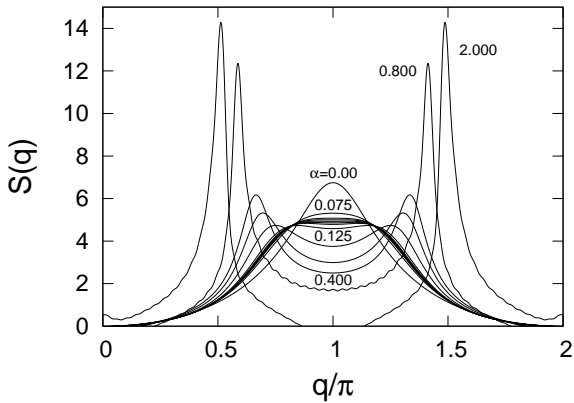


FIG. 18: The momentum space correlation function  $S(q)$  for  $\beta = 0.3$  and various values of  $\alpha$ . We find a Lifshitz point at  $\alpha_L(\beta = 0.3) = 0.095(2)$ .

### C. Results: $-1 < \beta < 0$

As we have shown previously, the effect of a large negative  $\beta$  is to form dimers between neighboring spins even in the presence of a finite  $\alpha$  the spin chain is spontaneously dimerized. When the system is in close proximity to the dimer phase it is possible for the model to experience short range dimer order, similar to the disorder point, this will appear in the correlation function as a finite dimerization on top of the OZ form

$$C_D(x) \propto (1 + \delta(\alpha, \beta)(-1)^x)C_{OZ}(x), \quad (9)$$

in the following we will use the criteria  $\delta(\alpha, \beta) > 0$  to define short range dimer order. We define the lower and upper dimerization cross over lines as  $\alpha_d^l(\beta)$  and  $\alpha_d^u(\beta)$  respectively, where  $0 < \delta(\alpha, \beta) < 1$  for  $\alpha_d^l(\beta) < \alpha < \alpha_d^u(\beta)$ . For  $\alpha > \alpha_d^u(\beta)$  the correlation function can be fit using the standard OZ form in equation (7).

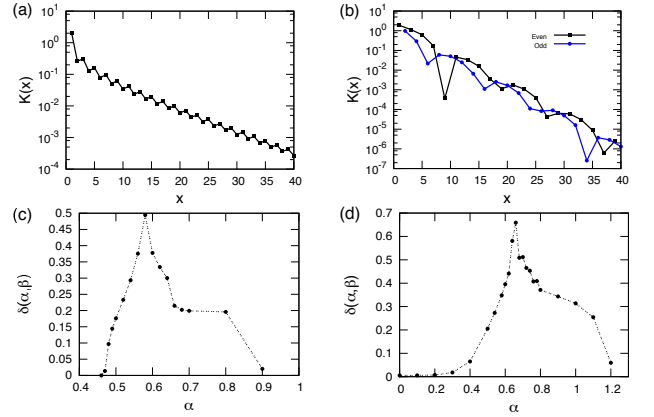


FIG. 19: (Color online) The real space correlation function  $C(x)$ , plotted in terms of  $K(x) \equiv C(x)(-1)^x \sqrt{x}$  for  $\beta = -0.2$  and  $\alpha = 0.50$  in the dimer phase (a) with  $q(\alpha, \beta) = \pi$  and  $\alpha = 0.80$  in the incommensurate dimer phase (b) plotted for even (black) and odd (blue) values of  $x$  to show clearly finite dimerization on top of an OZ form with  $q(\alpha, \beta) > \pi$ . The dimerization  $\delta(\alpha, \beta)$  for  $\beta = -0.2$  (c) and  $\beta = -0.3$  (d) as a function of  $\alpha$ . We see the dimerization rises continuously as we cross  $\alpha_d^l(\beta)$  and then has a cusp at the dL line which then decreases in the incommensurate dimer phase. Where  $\delta(\alpha, \beta)$  is going to zero defines the cross over line  $\alpha_d^u(\beta)$  between the incommensurate dimer phase and the NNN AKLT phase.

#### 1. Disorder, Lifshitz, and Dimerization Lines

In the range  $-0.125 \lesssim \beta < 0$ , fixing  $\beta$  and tuning  $\alpha$  the model continues to pass through the disorder, Lifshitz and transition lines at  $\alpha_d(\beta) < \alpha_L(\beta) < \alpha_T(\beta)$  respectively, each point has the same properties as described for  $\beta > 0$ . The only distinction is due to a negative  $\beta$  we find  $\alpha_d(\beta) = \alpha_d^l(\beta)$ , i.e. upon crossing the disorder line, we find a short range incommensurate dimerized phase, with both  $q(\alpha, \beta) > \pi$  and  $0 < \delta(\alpha, \beta) < 1$ . When both

$q(\alpha, \beta)$  and  $\delta(\alpha, \beta)$  are small it is difficult to accurately determine a precise value of the dimerization, however it is clear when the standard OZ form is a good fit and we use this to determine  $\alpha_\delta^u(\beta)$ , which in this range of  $\beta$  we find  $\alpha_\delta^u(\beta) < \alpha_L(\beta)$ .

## 2. Cross Over from the Dimer to the NNN AKLT phases: Disorder, Lifshitz and Dimerization lines

As we have discussed previously, for the range  $-0.15 \lesssim \beta < 1$  the transition line line lies above the disorder and Lifshitz lines in the  $\beta - \alpha$  phase diagram. However, for  $-1 \leq \beta < -0.15$  we find the critical line has passed below the disorder and Lifshitz lines and in fact within this range we find the disorder and Lifshitz points have merged to become a single line, i.e.  $\alpha_c(\beta) < \alpha_d(\beta) = \alpha_L(\beta) \equiv \alpha_{dL}(\beta)$ , which we will refer to as the dL line. The dL line is now a cross over between the dimerized phase and an incommensurate dimerized phase, since this is not a true transition phase transition we conclude that the incommensurate order is short ranged. Upon further increasing  $\alpha$  we find the dimerization in the correlation function  $\delta(\alpha, \beta)$  goes to zero (see figure 19) and the dimer order parameter becomes vanishingly small in the thermodynamic limit (see figures 11a and 12a). We see no signature of a phase transition in the correlation length and the edge excitations are gapped out in both phases. Therefore, for this range of  $\beta$  we use the line  $\alpha_\delta^u(\beta)$  to define the cross over into the NNN AKLT phase. As our results show, the spontaneously dimerized phase is smoothly connected to the NNN AKLT phase, since they both break the same symmetry, namely, the translational symmetry.

## D. Full Phase Diagram

We are now in a position to construct the phase diagram in terms of both short and long range order. We find a variety of short range ordered phases as a result of the interplay between frustration and the biquadratic interaction. The phases are defined below and are shown in the quantitative phase diagram in figure 20.

- SA-C: Short range antiferromagnetic correlations, with a real space correlation function,  $C(x)$  well described by the OZ form of equation (7) with  $q(\alpha, \beta) = \pi$ . The momentum space correlation function,  $S(q)$  has a single peak at  $\pi$ .
- SA-ICR: Short range antiferromagnetic correlations with incommensurate correlations in real space.  $C(x)$  is well described by the OZ form with  $q(\alpha, \beta) > \pi$  and  $S(q)$  has a single peak at  $\pi$ . In this phase, the ground state is closest to the AKLT wave function ansatz.
- SA-ICM: Short range antiferromagnetic correlations with incommensurate correlations in both, real and momentum space.  $C(x)$  is well described by the OZ form with  $q(\alpha, \beta) > \pi$ .  $S(q)$  has two symmetric peaks at an

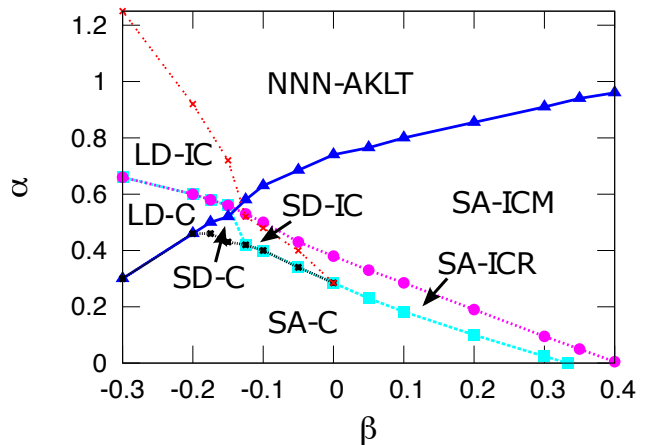


FIG. 20: (Color online) Phase diagram obtained with DMRG, each phase is described in the text. The disorder line  $\alpha_d(\beta)$  (cyan squares) and Lifshitz line  $\alpha_L(\beta)$  (magenta circles) intersect the critical line  $\alpha_T(\beta)$  (blue triangles) and become a single line in the symmetry broken phase. The lower disorder line  $\alpha_\delta^l$  (black x's) separates from the disorder line and becomes a true transition  $\alpha_c(\beta)$  for  $\beta \lesssim -0.2$ . Lastly, the red x's represent the cross over line to the NNN AKLT phase  $\alpha_\delta^u$  and the absence of dimerization. Note,  $\alpha_L(\beta = 0.4) = 0.005(1)$  and  $\alpha_L$  goes to zero at  $\beta = 0.43806(4)$  (Ref. 39)

incommensurate wave vector, see figure 18.

- SD-C: Short range dimer correlations with commensurate correlations in real and momentum space.  $C(x)$  is reasonably fit with the dimerized OZ, equation (9) with  $\delta(\alpha, \beta) > 0$  and  $q(\alpha, \beta) = \pi$ . The momentum space correlation function,  $S(q)$  has a single peak at  $\pi$ .
- SD-IC: Short range dimer correlations with incommensurate corrections in real space.  $C(x)$  is reasonably fit with the dimerized OZ, equation (9) with  $\delta(\alpha, \beta) > 0$  and  $q(\alpha, \beta) > \pi$ . The momentum space correlation function,  $S(q)$  has a single peak at  $\pi$ .
- LD-C: Translational symmetry broken, the dimer order parameter is finite in the thermodynamic limit,  $C(x)$  is reasonably fit with the dimerized OZ, equation (9) with  $\delta(\alpha, \beta) > 0$  and  $q(\alpha, \beta) = \pi$ . The ground state energy is very close to the dimer wave function ansatz and  $S(q)$  has a single peak at  $\pi$ .
- LD-IC: Translational symmetry broken, with short range incommensurate correlations, the dimer order parameter is finite in the thermodynamic limit,  $C(x)$  is reasonably fit with the dimerized OZ, equation (9) with  $\delta(\alpha, \beta) > 0$  and  $q(\alpha, \beta) > \pi$ .  $S(q)$  has two symmetric peaks at an incommensurate wave vector.
- NNN AKLT: Translational symmetry broken, with a negligible dimer order parameter in the thermodynamic limit.  $C(x)$  is well described by the OZ form with  $q(\alpha, \beta) > \pi$ .  $S(q)$  has two symmetric peaks at an incommensurate wave vector that approaches  $\pi/2$  for large values of  $\alpha$ .

## VI. DISCUSSION

It is interesting to contrast our work with a previous study in Ref. 40, in which the translational symmetry of the lattice is broken by construction, by adding the term  $\sum_i ((-1)^i \delta) \mathbf{S}_i \cdot \mathbf{S}_{i+1}$  to the nearest neighbor Heisenberg interaction in the Hamiltonian (1) with  $\beta = 0$ . As a result, a dimerized phase was found for sufficiently large  $\delta$ , which appeared to be smoothly connected to the NNN AKLT phase<sup>11,12</sup>. In the present study on the other hand, the translational symmetry is broken spontaneously, however we similarly find that the dimerized and NNN AKLT phases are most likely smoothly connected, and we refer to them jointly as the translational symmetry broken phase (TSBP).

In this work, we have not computed the string order parameter from DMRG because of the technical difficulties of the calculation. Instead, we have tracked the existence or absence of the edge excitations to monitor the topological nature of the ground state. We have found that the edge excitations become gapped out as one crosses the critical line  $\alpha_c(\beta)$  (or first-order transition line  $\alpha_T(\beta)$ ) from below, and the edge wavefunction hybridizes with the bulk states. As a result, we conclude that the critical (transition) line separates the topologically nontrivial Haldane phase from the topologically trivial TSBP phase. It has recently been shown by Gu and Wen<sup>64</sup> that the Haldane phase for spin-1 chain is an example of the symmetry-protected topological phase (the symmetries are time-reversal, parity, and translational invariance). This result was generalized to the case of odd-integer spin chains ( $S = 1, 3, 5 \dots$ ) by Pollmann *et al.* in Ref. [65], who also showed that the dimer state is, by contrast, topologically trivial. Interestingly, the even-integer spin chains do not possess this property, as the authors argue that the Haldane phase is topologically trivial in this case<sup>65</sup>. Our calculations indicate that that the NNN-AKLT phase is smoothly connected to the dimer phase and is therefore topologically trivial, as is the dimer phase<sup>65</sup>. However more work along these lines is needed, and it would be instructive to compute the evolution of the string order parameter across both the critical  $\alpha_c(\beta)$  and transition  $\alpha_T(\beta)$  lines. It will be interesting to see whether the string order parameter goes to zero continuously across the critical line, or if it still jumps similar to the case of  $\beta = 0$ , as earlier DMRG calculations indicate<sup>11,12</sup>.

Intriguingly, we find that the topological phase transition from Haldane into the TSBP phase can occur both with (for  $\beta < \beta^*$ ) and without (for  $\beta > \beta^*$ ) closing of the bulk gap at the transition. While the conventional wisdom based on the bulk-edge correspondence dictates that the bulk gap must close at such a transition, there is a number of examples found recently in which the bulk gap can remain finite, provided the symmetry of the system changes across the topological transition<sup>66</sup>. This argument provides solid footing for our findings in the region  $\beta > \beta^* \approx -0.2$ , where the DMRG calculated bulk

gap remains finite across the  $\alpha_T(\beta)$  line, in agreement with earlier DMRG calculations at  $\beta = 0$ <sup>11,12</sup> and field-theoretical results<sup>13</sup>.

We have established the existence of both a critical line  $\alpha_c(\beta)$  and transition line  $\alpha_T(\beta)$  in the phase diagram Fig. 2. Crucially, crossing a line of the phase boundary does not require fine-tuning of both  $\alpha$  and  $\beta$  parameters, as opposed to a single point in the phase diagram. Experimentally, both  $\alpha$  and  $\beta$  interactions are generically present in the system, and our results thus raise an exciting prospect of being able to observe the critical/transition line experimentally. Therefore, we expect that a signature of the transition should be accessible in an experiment, provided the compound is frustrated enough. This is in contrast to, say, the TB point, or the ULS point, which would require fine tuning and therefore are much more difficult to observe experimentally.

This manuscript has focused on the parameter range  $\beta < 1$  and  $\alpha > 0$ . It will be very interesting to consider the effect of frustration on the ULS point and the gapless<sup>25</sup> antiferro-quadrupolar phase for  $\beta > 1$ . It is a natural question to ask whether this gapless phase will still exist for a finite  $\alpha$ , and if so, whether there is a direct transition between this phase and the NNN-AKLT phase on the right-hand side of the schematic phase diagram of figure 2. In addition, the ULS point ( $\beta = 1, \alpha = 0$ ) is known to be described by the  $SU(3)_{k=1}$  CFT with gapless modes at  $q = 0, \pm 2\pi/3$  (that show up clearly in  $S(q)$ , see Ref. 39). It will be very interesting to consider perturbations (as a result of a finite  $\alpha$ ) to the ULS point, similar to the field theoretical approach in section III A. Also, in this case the model has already passed through a disorder and Lifshitz point due to the large positive  $\beta$ , and we therefore expect the peaks of the spin structure factor  $S(q)$  to shift continuously with increasing  $\alpha$ , from  $\pm 2\pi/3$  to  $\pm \pi/2$ .

## VII. CONCLUSIONS

By combining field theoretical arguments, DMRG calculations, and a variational wave function ansatz we have been able to construct the phase diagram of the frustrated antiferromagnetic biquadratic spin-1 chain in the range  $\beta < 1$  and  $\alpha \geq 0$ . In particular, using the non-Abelian bosonization and DMRG, we have demonstrated the existence of a critical line that terminates at a multicritical endpoint  $\Omega = (\beta^*, \alpha^*)$ , with approximate bounds  $-0.2 < \beta^* < -0.15$  and  $0.47 < \alpha^* < 0.53$ . We conjecture that the conformal field theory describing the low-energy excitations at the  $\Omega$  point is distinct from previously known gapless points in the phase diagram, and is characterized by the Wess-Zumino-Witten theory  $SU(2)_4$  with central charge  $c = 2$ . To the right of the critical endpoint (for  $\beta > \beta^*$ ), the critical line becomes a line of first order phase transitions, corroborating earlier DMRG calculations<sup>11,12</sup> at  $\beta = 0$ . This critical/first-order transition line separates the topologically non-trivial Haldane

(AKLT) phase from the topologically trivial translational symmetry broken phase (TSBP). The TSBP is divided into the dimer and so-called NNN AKLT phases, which are smoothly connected by a crossover through an incommensurate dimer phase.

These findings are corroborated by DMRG calculations of the bulk and edge gaps, the spin-spin correlation length, the entanglement entropy, the ground state energy, and the dimer order parameter. In addition, we have used the matrix-product state variational wave function as an intuitive guide to the DMRG calculations, allowing us to determine the character of the ground state wave function in each phase.

Extending earlier DMRG work by other authors, we show the existence of two incommensurate crossovers inside the Haldane phase: the Lifshitz transition  $\alpha_L$  and the so-called disorder transition of the first kind  $\alpha_d$ , marking incommensurate correlations in momentum and real space, respectively. Whereas earlier, these two transitions have been only characterized at isolated points ( $\alpha = 0$  or  $\beta = 0$ ), here we show that they stretch across the entire  $(\alpha, \beta)$  phase diagram. Outside of the Haldane phase (inside the TSBP), these two lines merge into a single incommensurate-to-commensurate transition line. This behavior is similar to that seen in classical frustrated two dimensional spin models. Intriguingly, we find that the point of this merging coincides, within the precision of our numerical calculations, with the multicritical end-point  $\Omega$ .

## VIII. METHODS

### A. DMRG

For the DMRG calculations presented here we are using the open source POWDER DRMG code<sup>42</sup>. We keep  $M = 200$  states, for ground state energy calculations we extrapolate in system size for  $L = 40, 50, 60, 70, 80, 90$ , and 100. We determine the ground state energy, the gap and the dimer order parameter in the thermodynamic limit by fitting to quadratic polynomials

$$f(L) = f^\infty + a_f/L + b_f/L^2. \quad (10)$$

$f$  is quantity being extracted to the the thermodynamic limit with the extrapolated value  $f^\infty$ . For  $\beta > 0$  we present correlation functions for chain lengths  $L = 100$  and for  $\beta < 0$  we used  $L = 80$ , such that the truncation error is at most  $10^{-9}$  (when we are away from the critical line) and perform 5 finite size DMRG sweeps such that the results are well converged. In the vicinity of the critical and transition lines convergence is quite poor and the truncation error can be as large as  $10^{-7}$ .

### B. Conformal Field Theory

In this section, we provide a more rigorous field theoretical argument regarding the statement made in Section III A 2 about the conformal field theory  $SU(2)_4$  which, we conjecture describes the critical end-point  $\Omega$  in the  $(\alpha, \beta)$  phase diagram (see Figs. 2, 3).

We start from the representation of the spin-1 Hamiltonian in terms of two coupled chains as in Eq. (3). Even though in this work we are interested in an antiferromagnetic spin chain, it is instructive to consider the case of a ferromagnetic interchain coupling  $J_\perp$  (recall that  $J_\perp$  in Eq. (3) corresponds to  $J_1$  in the original model Eq. 1). Let us consider the dimerized phase above the solid line in the phase diagram Fig. 3. Then, for sufficiently large ferromagnetic  $J_\perp$ , the alternating rungs will form spin-triplet dimers as in Fig. 6b. The model is then equivalent to a spin  $S = 2$  chain, in the limit when the coupling  $J_2$  is not too large. The question now is: what conformal field theory describes a critical point in this  $S = 2$  model?

Because of the  $SU(2)$  spin symmetry, the sought theory is most likely the WZW  $SU(2)_k$  at level  $k$ . It is well established that the Kac-Moody currents  $J_L^a, J_R^a$  of such a theory can be expressed as bilinears in terms of free (albeit nonlocal) fermionic degrees of freedom<sup>62,63</sup>. In particular,  $J_R^a$  is expressed through the right (R) movers:  $J_R^a = \sum_n : \psi_{R,\alpha,n}^\dagger \tau_{\alpha\beta}^a \psi_{R,\beta,n} :$ , with a similar expression for  $J_L^a$  in terms of left movers, where  $\tau^a$  are the generators of the  $SU(2)$  group (Pauli matrices). Consider now 2 neighboring effective spins  $S = 2$ : we need  $k = 4$  “flavours” of fermions to describe all the degrees of freedom. Such a free fermionic theory has  $U(k) \times SU(N)$  symmetry. Using a group identity  $U(k) \times SU(N) = U(1) \times SU(N) \times SU(k)$ , one can represent the fermionic operators in terms of the product of an  $SU(2)_k$  spin WZW field, an  $SU(k)_2$  flavour WZW field, and a free boson corresponding to the charge  $U(1)$  field<sup>50,51</sup>. Since we are dealing with a charge insulator, the  $U(1)$  field is gapped. The flavour field corresponds to the “valley”  $SU(k)$  symmetry and is of no consequence (in fact, it can be gapped out by introducing perturbations to the model<sup>63</sup>). The only remaining gapless field describes the low-energy spin-2 degrees of freedom in terms of the  $SU(2)_{k=4}$  WZW theory. This is an example of a more general proposal by Affleck<sup>52</sup> that certain multicritical points of the spin- $S$  Heisenberg model are described by  $SU(2)_k$  WZW theory at level  $k = 2S$ .

As noted in Section III A 2, the  $SU(2)_4$  theory has one relevant field with scaling dimension  $\Delta_1 = 2/3$ , expressed in terms of the bilinear of primary operators, as well as two marginal fields – one relevant and one irrelevant. It is instructive to analyze what those fields correspond to in terms of the original spin model. For this, let us consider in more detail the two coupled spin chains in Eq. (3). Each spin-1 chain in (3) can be described by the WZW theory with perturbation as in Eq. (2):

$$\mathcal{L} = \mathcal{L}_1^{\text{WZW}} + \mathcal{L}_2^{\text{WZW}} + \mathcal{L}_\perp + \{\text{perturbations}\}. \quad (11)$$

Following Allen and Sénéchal<sup>48</sup>, the coupling between the

two chains can be described in the language of the aforementioned primary fields  $\hat{g}^a$  and the conformal currents  $J^a, \bar{J}^a$  of each chain:

$$\begin{aligned} \mathcal{L}_\perp = & \lambda_2(J_1^a J_2^a + \bar{J}_1^a \bar{J}_2^a) + \lambda_3(J_1^a \bar{J}_2^a + \bar{J}_1^a J_2^a) \\ & + \rho [g_1^a (\partial_x g_2^a) - (\partial_x g_1^a) g_2^a]. \end{aligned} \quad (12)$$

The last term, referred to as the *twist term* is strongly relevant and is highly nontrivial to analyze due to its non-vanishing conformal spin. The bosonization treatment by Allen and Sénéchal<sup>48</sup> showed that it is responsible for the onset of incommensurability in the spin-spin correlations as  $J_\perp$  increases. It is this relevant term that leads to the dimer or NNN-AKLT phase and opens up the spectral gap, and we can therefore relate it with the corresponding *relevant* bilinear of the primary operators in the effective  $SU(2)_4$  theory.

The first two terms in Eq. (12) have a scaling dimension  $\Delta = 2$  and are therefore marginal. Their effect depends on the sign of the coupling constants: both  $\lambda_2$  and  $\lambda_3$  are proportional to  $J_\perp \equiv J_1$  and become *relevant* for an antiferromagnetic  $J_\perp$ . Indeed, in this case the lowest-lying excitations are the rung triplets on the zigzag chain in Fig. 6 and they cost an energy  $\sim J_\perp$  for large positive interchain coupling<sup>48</sup>. In the language of the effective  $S = 2$  model, this is the *marginally relevant* field of the  $SU(2)_4$  model.

Finally, there remains a *marginal* current bilinear in the  $SU(2)_4$  model. It corresponds to the marginally irrelevant current bilinear ( $\bar{J}_n J_n$ ) in each of the individual chains ( $n = 1, 2$ ), which only becomes marginally relevant if the intra-chain interaction  $J_2$  is ferromagnetic. In this work, we only consider antiferromagnetic  $J_2$ , so this term remains *marginally irrelevant*.

To conclude, we have shown that the spin-1 chain exhibits emergent  $S = 2$  excitations and provided those are gapless, they are described by the critical  $SU(2)_4$  conformal field theory. We have identified the physical meaning of various relevant and marginal operators of this theory by establishing their correspondence with the fields of the two coupled spin-chain model in Eq. (3).

### C. Variational MPS Wave Function

Matrix Product States (MPS) have emerged as a powerful tool for analytic studies of correlated quantum systems. The representation of the exact ground state of the one-dimensional AKLT state using MPS<sup>18</sup> led to in-depth studies of these states<sup>28</sup>, which pertinent to the present case, were subsequently used for analytical calculations for spin-1 chains, e.g. in Refs.<sup>11,12,29,30,32,33,36</sup>. In this tradition, we construct a variational MPS wavefunction first introduced in Refs. 11,12, to study the ground state and low-lying excitations of Hamiltonian (1), depicted in Fig. 21. We first consider the MPS representation of the

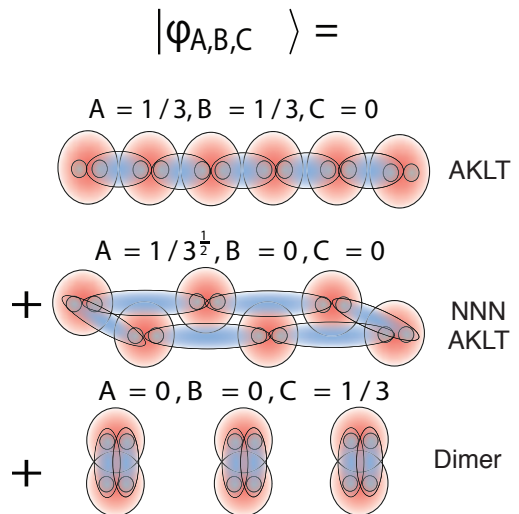


FIG. 21: The variational Matrix Product State (MPS) wavefunction is constructed using three states, AKLT, NNN-AKLT, and dimer, which can be represented individually as MPSs, see Eq. (14). Parameters  $A, B, C$  can be chosen to interpolate between the three states, which can each be recovered by a special choice of parameters shown in the figure above.

AKLT wavefunction,  $|\psi\rangle = \text{Tr} [g_1 \cdot g_2 \cdot g_3 \cdot \dots \cdot g_M]$  with

$$g_{\text{AKLT}} = \frac{1}{\sqrt{3}} \begin{pmatrix} |0\rangle & -\sqrt{2}|+\rangle \\ \sqrt{2}|-\rangle & -|0\rangle \end{pmatrix} \quad (13)$$

where the matrices  $g_i$  at sites  $i = 1, 2, \dots, M$  are identical due to translational invariance, and each is constructed in the  $S = 1$  local spin basis at site  $i$ ; the construction can be understood by first realizing that the AKLT Hamiltonian can be rewritten as a sum of projectors onto  $S = 2$  in the space of spins at adjacent sites  $i, i+1$ . This implies that the ground state must have total spin  $S_{i,i+1} \neq 2$  at sites  $i, i+1$ . Such a state can be conceptualized by introducing a set of auxiliary  $S = 1/2$  spins at each site of the chain (see Fig. 1), and preparing each adjacent pair of  $S = 1/2$  spins in a singlet. It is simple to check that the sequence of matrices  $g$  in Eq.(13) encapsulates this structure.

#### 1. Variational approach to the ground state

The AKLT MPS is a good approximation to the true ground state of  $H$  in the vicinity of the AKLT point  $\beta = 1/3, \alpha = 0$  (see<sup>11,18</sup>). To go beyond this regime we use the physical insight that next-nearest neighbor interactions dominate over nearest-neighbor ones for large positive  $\alpha$  and that the system dimerizes for large negative  $\beta$ . Thus, we introduce the “next-nearest-neighbor” AKLT and the “dimerized” MPS which contain these two essential effects, respectively. In the spirit of Refs. 11,12 we construct a variational MPS which interpolates be-

tween the AKLT MPS and the two additional MPS described above (see Fig. 21):

$$|\phi_{A,B,C}\rangle = \text{Tr}[\Gamma_{1,2}\Gamma_{3,4}\Gamma_{5,6}\dots\Gamma_{M-1,M}], \quad (14)$$

$$\Gamma_{1,2} = \sum_{i,j} |t_{1i}, t_{2j}\rangle \left[ A\delta_{i,j}\mathbb{1}_4 + iB\varepsilon_{ijk}(\sigma_k \otimes \mathbb{1}_2) + iC(\sigma_i \otimes \sigma_j) \right] \quad (15)$$

where  $A, B, C$  determine the relative weights of the three candidate MPS states,  $\sigma_i$  are usual  $2 \times 2$  Pauli spin matrices,  $\varepsilon_{ijk}$  is the Levi-Civita symbol, and the matrices  $\Gamma_{i,i+1}$  are identical due to translational invariance. Note that it is more convenient to construct the variational state in the space of 2 adjacent spins, concretely  $|t_{1i}t_{2j}\rangle$  is the decoupled basis of  $S = 1$  spins at sites 1,2, with  $|t_i\rangle$  expressed in the Cartesian basis  $i = (x, y, z)$ , i.e.

$$S_x|t_x\rangle = 0, \quad S_y|t_y\rangle = 0, \quad S_z|t_z\rangle = 0. \quad (16)$$

Choosing parameters  $A = B = 1/3, C = 0$  yields the AKLT MPS, while the completely dimerized state is given by  $A = 1/\sqrt{3}, B = C = 0$ , and the NNN-AKLT state corresponds to  $A = B = 0, C = 1/3$ . The crucial point is that optimal  $A, B, C$  can be determined by minimizing the energy  $\langle \phi | H | \phi \rangle$ .

It is most convenient to compute expectation values of local observables in the MPS using the transfer matrix technique of Refs.<sup>11,12,30,31</sup>. For example the total energy can be decomposed into a sum of local operators  $H = \sum_i h_{i,i+1}^{nn} + h_{i,i+2}^{nnn}$  which can then individually be evaluated in state  $|\phi\rangle$ . The essential steps involve computing and diagonalizing the transfer matrix  $G = \Gamma^\dagger \otimes \Gamma$ , a  $16 \times 16$  matrix; all operator expectation values will involve traces over chains of the matrix  $G$  sandwiched between operators, e.g.

$$\langle O^{(1)}(i)O^{(2)}(j) \rangle = \text{Tr}[G_1 \dots O^{(1)}(i)G_{i+1} \dots O^{(2)}(j) \dots G_M], \quad (17)$$

which in the thermodynamic limit will be dominated by the largest eigenvalue of  $G$  leading to

$$\lim_{M \rightarrow \infty} \langle O_i O_j \rangle = \lambda_{\max}^M \sum_m \lambda_m^{j-i-1} (U^\dagger O^{(1)} U)_{1,m} (U^\dagger O^{(2)} U)_{m,1}, \quad (18)$$

where  $\lambda_{\max}$  is the largest eigenvalue of  $G$ .  $U$  diagonalizes  $G$ , i.e.  $U^\dagger G U = \lambda_i \delta_{ij}$  with the convention  $\lambda_1 = \lambda_{\max}$ . We find it convenient to normalize the maximal eigenvalue of  $G$  to unity which leads to a constraint<sup>11,12</sup> on  $A, B, C$ :

$$3A^2 + 6B^2 + 9C^2 = 1. \quad (19)$$

Observables including two-point correlation functions can be calculated either directly using Eq. (18) or by straightforward generalizations. Thus within the variational approach we can calculate the ground state energy as well as correlation functions.

## 2. Variational approach to the low energy excitations

It is also possible to approximate the low lying excitations above the ground state within the MPS framework<sup>12,34</sup>. The idea shadows the single mode approximation used to obtain dispersions for spin chains<sup>35</sup>: excitations are constructed by adding traveling ‘‘defects’’ or solitons<sup>12,34</sup> to the ground state,

$$|E(k)\rangle = \sum_n e^{ink} \text{Tr}[g_1 \otimes g_2 \otimes \dots c_n \otimes \dots g_M], \quad (20)$$

where  $c_n$  is a defect at site  $n$ , which e.g. in the AKLT case is given by

$$c_n = \sigma^{\pm,z} g_{\text{AKLT}}. \quad (21)$$

Note that there are three possible excitation modes which can be generated by the appropriate spin defect; here it corresponds to choosing one of the three Pauli sigma matrices in the spherical basis  $(z, +, -)$ <sup>12</sup>. Due to the rotational symmetry of our model, the three dispersion modes are degenerate.

To gain intuition into the structure of the low-energy excitations in the three phases depicted in Fig. 13, within the approximation of Eq. (20) we calculated the dispersion  $\varepsilon(k)$  of the AKLT MPS state which we obtained in closed form (see also Refs. 11,12):

$$\begin{aligned} \varepsilon(k) = & \frac{14}{9} + \frac{26}{27}\alpha + \frac{160\alpha - 18}{27} \cos(k) - \frac{14}{9}\alpha \cos(2k) \\ & + \left(2 - \frac{26}{3}\alpha\right) \frac{3 + 5 \cos(k)}{5 + 3 \cos(k)} + \frac{2}{9}\beta(13 + 9 \cos(2k)). \end{aligned} \quad (22)$$

By choosing values of  $\alpha, \beta$  lying in the relevant regions of the phase diagram in Fig. 13, we obtain dispersion curves which we argue characterize the low energy excitations of the AKLT, NNN AKLT, and dimer phases. Thus we present the spin dispersion within this approximation for representative values of  $\alpha, \beta$  in Fig. 22. The justification for using the AKLT MPS ground state as the starting point to explore dispersions in neighboring phases is provided by the fact that even within our variational approach, the *ground states* in a region of the NNN-AKLT and dimer phases are well approximated by the AKLT state (see Fig. 23).

## IX. ACKNOWLEDGEMENTS

We would like to thank M. Kormos, M. Foster, Q. Si, I. Affleck, S. White, T. Senthil, S. Deppenbrock, V. Oganesyan, C. Broholm, M. Barkeshli, and Y. Z. Chou for useful discussions. We would especially like to thank Matteo Rizzi for his detailed help in using the POWDER DMRG code. The calculations have been performed on Rice University Data Analysis and Visualization Cyberinfrastructure funded by the NSF under grant

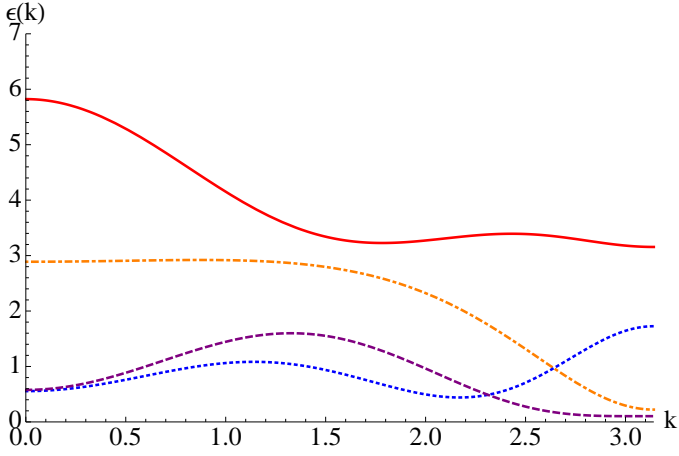


FIG. 22: (Color online) Approximate dispersion curves  $\varepsilon(k)$  calculated for representative choices of couplings  $\alpha, \beta$  within the single mode or “crackion” approach. The dotted line (blue) is evaluated for  $\alpha = 0, \beta = 0$ , is shown for reference and captures the physics deep within the AKLT phase; the dashed-dotted (orange) line corresponds to  $\alpha > 0$  and approximates the excitations in the NNN-AKLT phase; the dashed (purple) line corresponds to  $\beta < 0$ , the dimer phase, and the solid (red) line corresponds to  $\beta > 0$ . We observe a shift in the minimum of the dispersion curve away from the AKLT phase, in which the minimum occurs at  $k = \pi$  as we tune  $\alpha, \beta$ , see also Fig. 18.

OCI-0959097. This work was supported in part by the East-DeMarco fellowship (JHP) and Welch Foundation grant C-1818 (AHN).

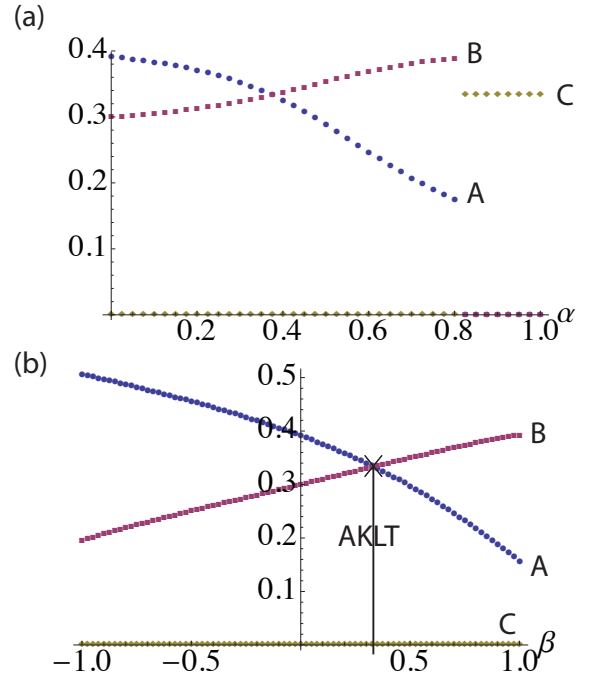


FIG. 23: (Color online) Values of  $A, B, C$  (respectively blue circles, red squares, yellow diamonds) shown as next-nearest neighbor coupling  $\alpha$  and biquadratic coupling  $\beta$  are tuned across the pure Heisenberg coupling point  $\alpha = 0, \beta = 0$  deep inside the Haldane phase. (a) For a fixed  $\beta = 0$  we show  $A, B, C$  as a function of  $\alpha$ ; (b) For a fixed  $\alpha = 0$  we show  $A, B, C$  as a function of  $\beta$  – the point  $\beta = 1/3$  corresponds to the AKLT point for which the AKLT MPS state is the exact ground state (corresponding to  $A = B = 1/3, C = 0$ ). Note that, within our approximation, the AKLT state also coincidentally describes the point  $\alpha = 0.374, \beta = 0$  shown in (a). Moreover, we observe that the parameters  $A, B, C$  are “close” to the AKLT values for a large portion of the phase diagram (with the exception of regions deep in the NNN-AKLT phase  $\alpha \gtrsim 0.8$ ).

- <sup>1</sup> *Frustrated Spin Systems*, H. T. Diep (Ed.), World Scientific (2005).
- <sup>2</sup> Shaolong Ma, Collin Broholm, Daniel H. Reich, B. J. Sternlieb, and R. W. Erwin, Phys. Rev. Lett. **69**, 3571-3574 (1992).
- <sup>3</sup> M. Kenzelmann, R. A. Cowley, W. J. L. Buyers, Z. Tun, R. Coldea and M. Enderle, Phys. Rev. B **66**, 024407 (2002).
- <sup>4</sup> M. Kohgi, K. Iwasa, J.-M. Mignot, A. Ochiai and T. Suzuki, Phys. Rev. B **56**, R11388 (1997).
- <sup>5</sup> K. Yip, Phys. Rev. Lett. **90**, 250402 (2003).
- <sup>6</sup> A. Imambekov, M. Lukin, and E. Demler, Phys. Rev. A **68**, 063602 (2003).
- <sup>7</sup> J. J. Garcia-Ripoll, M. A. Martin-Delgado, and J. I. Cirac, Phys. Rev. Lett. **93**, 250405 (2004).
- <sup>8</sup> M. Inui, S. Doniach, and M. Gabay, Phys. Rev. B **38**, 6631-6635 (1988).
- <sup>9</sup> R. Yu, Z. Wang, P. Goswami, A. Nevidomskyy, Q. Si and E. Abrahams, Phys. Rev. B **86**, 085148 (2012).
- <sup>10</sup> F. D. M. Haldane, Phys. Lett. **93A**, 464 (1983); Phys. Rev. Lett. **50**, 1153 (1983).
- <sup>11</sup> A. Kolezhuk, R. Roth and U. Schollwöck, Phys. Rev. Lett. **77** 5142 (1996).
- <sup>12</sup> A.K. Kolezhuk, R. Roth, and U. Schollwöck, Phys. Rev. B **55**, 8928 (1997).
- <sup>13</sup> D. Allen and D. Sénéchal, Phys. Rev. B **51**, 6394 (1995).
- <sup>14</sup> T. Giamarchi, *Quantum Physics in One Dimension* (Oxford Univ. Press, 2004).
- <sup>15</sup> M. den Nijs and K. Rommelse, Phys. Rev. B **40**, 4709 (1989).
- <sup>16</sup> T. Kennedy and H. Tasaki, Phys. Rev. B **45**, 304 (1992).
- <sup>17</sup> T. Kennedy, J. Phys. Condens. Matter **2**, 5737 (1990).
- <sup>18</sup> I. Affleck, T. Kennedy, E. H. Lieb, and H. Tasaki, Phys. Rev. Lett. **59**, 799802 (1987); Commun. Math. Phys. **115**, 528 (1988).
- <sup>19</sup> M. N. Barber and M. T. Batchelor, Phys. Rev. B **40**, 4621 (1989).
- <sup>20</sup> A. Klümper, Europhys. Lett. **9**, 815 (1989).
- <sup>21</sup> Y. Xian, Phys. Lett. A **183**, 437 (1993).
- <sup>22</sup> L. A. Takhtajan, Phys. Lett. **87A**, 479 (1982).
- <sup>23</sup> H. M. Babudjian, Phys. Lett. **90A**, 479 (1982).
- <sup>24</sup> I. Affleck and F. D. M. Haldane, Phys. Rev. B **36**, 5291-5300 (1987).
- <sup>25</sup> A. Läuchli, G. Schmid, and S. Trebst, Phys. Rev. B **74**, 144426 (2006).
- <sup>26</sup> G. V. Uimin, JEPT Lett. **12**, 225 (1970); C. K. Lai, J. Math. Phys. **15**, 1675 (1974); B. Sutherland, Phys. Rev. B **12**, 3795 (1975).
- <sup>27</sup> E. S. Sørensen and A. P. Young, Phys. Rev. B **42** 754 (1990).
- <sup>28</sup> M. Fannes, B. Nachtergaele, and R. F. Werner, Europhys. Lett. **10** 633 (1989); Commun. Math. Phys. **144**, 443-490 (1992)
- <sup>29</sup> U. Schollwöck, Th. Joilcoeur and T. Garel, Phys. Rev. B **53** 3304 (1996).
- <sup>30</sup> A. Klümper, A. Schadschneider, J. Zittartz, Europhys. Lett., **24**, 293 (1993); Z. Phys. B **87**, 281 (1992); Europhys. Lett. **24**, 293 (1993).
- <sup>31</sup> Totsuka and M. Suzuki, J. Phys. Condens. Matter **7**, 1639 (1995).
- <sup>32</sup> A.K. Kolezhuk, H.J. Mikeska, S. Yamamoto, Phys. Rev. B, **55** R3336 (1997).
- <sup>33</sup> A.K. Kolezhuk, H.J. Mikeska, K. Maisinger, U. Schollwöck, Phys. Rev. B **59** 13565 (1999).
- <sup>34</sup> G. Fth and J. Slyom, Phys. Rev. B **47**, 872 (1993).
- <sup>35</sup> A. Auerbach, *Interacting electrons and quantum magnetism*, (Springer, 1994).
- <sup>36</sup> A.K. Kolezhuk, H.J. Mikeska, Phys. Rev. Lett., **80**, 2709 (1998).
- <sup>37</sup> S. R. White and D. A. Huse, Phys. Rev. B **48**, 3844 (1993).
- <sup>38</sup> M. Hagiwara, K. Katsumata, I. Affleck, B. I. Halperin, and J. P. Renard, Phys. Rev. Lett. **65**, 3181 (1990).
- <sup>39</sup> R. J. Bursill, T. Xiang, and G. A. Gehring, J. Phys. A Math. Gen. **28**, 2109 (1995).
- <sup>40</sup> S. K. Pati, R. Chitra, D. Sen., S. Ramasesha, and H. R. Krishnamurthy, Journal of Physics: Cond. Matt. **9**, 219, (1997).
- <sup>41</sup> U. Schollwöck Rev. Mod. Phys. **77**, 259 (2005).
- <sup>42</sup> G. De Chiara, M. Rizzi; D Rossini, S. Montangero, Journal of Computational and Theoretical Nanoscience, **5** ,1277 (2008).
- <sup>43</sup> N. D. Mermin and H. Wagner, Phys. Rev. Lett. **17**, 1133 (1966)
- <sup>44</sup> J. Cardy, *Scaling and Renormalization in Statistical Physics* (Camrbridge Univ. Press, 1996).
- <sup>45</sup> S. Yan, D. A. Huse, and S. R. White, Science **332**, 1173 (2011).
- <sup>46</sup> S. Depenbrock, I. P. McCulloch, and U. Schollwöck, Phys. Rev. Lett. **109**, 067201 (2012)
- <sup>47</sup> F. Anfuso and A. Rosch, Phys. Rev. B **76**, 085124 (2007).
- <sup>48</sup> D. Allen and D. Sénéchal, Phys. Rev. B **61**, 12134-12142 (2000).
- <sup>49</sup> A. B. Zamolodchikov, JETP Lett. **43**, 730-732 (1986).
- <sup>50</sup> I. Affleck, Nucl. Phys. B **265**, 409 (1986).
- <sup>51</sup> I. Affleck and A. W. W. Ludwig, Nucl. Phys. B **352**, 849 (1991); Phys. Rev. Lett. **67**, 3160 (1991).
- <sup>52</sup> I. Affleck, Phys. Rev. Lett. **56**, 746-748 (1986).
- <sup>53</sup> R. Thomale, S. Rachel, P. Schmitteckert, and M. Greiter, Phys. Rev. B **85**, 195149 (2012).
- <sup>54</sup> A.B. Zamolodchikov and V.A. Fateev, Sov. J. Nucl. Phys. **43**, 657-664 (1986).
- <sup>55</sup> D. Gepner and E. Witten, Nucl. Phys. B **278**, 493 (1986).
- <sup>56</sup> C. Holzhey, F. Larsen. amd F. Wilczek, Nucl. Phys. B **424**, 443 (1994).
- <sup>57</sup> P. Calabrese and J. Cardy, J. Stat. Mech: Theory and Experiment 2004, P06002 (2004).
- <sup>58</sup> T. Dombre and N. Read, Phys. Rev. B **39**, 6797 (1989).
- <sup>59</sup> P. Reed, J. Phys. A **27**, L69 (1994).
- <sup>60</sup> C. Itoi and M. Kato, Phys. Rev. B **55**, 8295 (1997).
- <sup>61</sup> A. Schmitt, K.-H. Mütter, M. Karbach, Y. Yu, and G. Müller, Phys. Rev. B **58**, 5498 (1998).
- <sup>62</sup> Ph. Di Francesco, P. Mathieu, and D. Sénéchal, *Conformal Field Theory*, Springer, New York (1997).
- <sup>63</sup> A. M. Tsvelik, *Quantum Field Theory in Condensed Matter Physics*, Cambridge Univ. Press (2007).
- <sup>64</sup> Z.-C. Gu and X.-G. Wen, Phys. Rev. B **80**, 155131 (2009).
- <sup>65</sup> F. Pollmann, E. Berg, A. M. Turner, and M. Oshikawa, Phys. Rev. B **85**, 075125 (2012).
- <sup>66</sup> M. Ezawa, Y. Tanaka, N. Nagaosa, Nature Scientific Reports **3**, 2790 (2013).